

# Connectomic analysis of the central complex in fruit fly larvae



**Laura Lungu**

*Supervisor: Professor Albert Cardona*

*Advisor: Dr. Marco Tripodi*

Department of Physiology, Development and Neuroscience  
University of Cambridge

This dissertation is submitted for the degree of  
*Doctor of Philosophy*

October 2025



I would like to dedicate this thesis to my loving parents . . .



## **Declaration**

I hereby declare that except where specific reference is made to the work of others, the contents of this dissertation are original and have not been submitted in whole or in part for consideration for any other degree or qualification in this, or any other university. This dissertation is my own work and contains nothing which is the outcome of work done in collaboration with others, except as specified in the text and Acknowledgements. This dissertation contains fewer than 60,000 words including appendices, bibliography, footnotes, tables and equations and has fewer than 150 figures.

Laura Lungu  
October 2025



## **Acknowledgements**

I would like to acknowledge Michael Clayton - help in data analysis and coding Nicolo Ceffa - help with light sheet imaging, flywork; Pedro Gomez Daniel Lalanti Venkat for teaching me foundations of flywork and immunostaining; Yije Yin - help with neurotransmitter volumes Sam Harris - for fly genetics and behavioural testing



## **Abstract**

### **Abstract**

In holometabolous insects such as the fruit fly *Drosophila melanogaster*, the brain central complex (CX) develops during metamorphosis and serves the adult stage. Whether a form of the CX exists in the brain of the evolutionarily novel larval stages is not known. Here, we analyzed the connectome of the larval brain and, on the basis of neuronal lineages, synaptic connectivity patterns, and anatomy, identified a putative larval CX, comprising 4 key neuropils: the protocerebral bridge (PB), the ellipsoid body (EB), the fan-shaped body (FB) and the noduli (NO). Consistent with our interpretation, we found in the larval brain synaptic connectivity patterns characteristic of the adult, including (i) visual input into the PB and EB; (ii) modulation of CX neuropil inputs by the mushroom body (MB); (iii) reciprocal connectivity between CX neuropils and select MB compartments; and (iv) strong connectivity between CX neuropils. While some neuronal lineages contributing to the larval CX do not contribute to the adult CX, many others are conserved. The characterization of a larval CX brings structure to largely unexamined larval brain circuits, linking with a vast body of literature, and will inform the design of experiments to probe larval brain function.



# Table of contents

<b>List of figures</b>	<b>xv</b>
<b>List of tables</b>	<b>xvii</b>
<b>1 Introduction</b>	<b>1</b>
1.1 Mapping brains - The Power of Connectomics . . . . .	1
1.2 The advantage of the <i>Drosophila</i> larva brain . . . . .	3
1.3 Navigation: Fundamental Across Species . . . . .	4
1.4 The Central Complex . . . . .	5
1.4.1 Central Complex across insects . . . . .	5
1.4.2 Central Complex of Adult <i>Drosophila</i> . . . . .	6
Protocerebral Bridge (PB) . . . . .	6
Ellipsoid Body (EB) . . . . .	7
Fan-Shaped Body (FB) . . . . .	8
Noduli (NO) . . . . .	8
Neuromodulatory neurons in the CX . . . . .	9
Mushroom Body and the CX . . . . .	10
1.5 Larval Central Complex as a research opportunity . . . . .	10
<b>2 Methods</b>	<b>15</b>
2.1 Reconstructing neurons in Electron Microscopy Volumes . . . . .	15
2.1.1 Connectome data . . . . .	15
2.1.2 Neurons Segmentation . . . . .	15
2.1.3 Data Analysis . . . . .	15
2.2 Identification of Central Complex Neuropils . . . . .	16
2.3 Identifying non-Mushroom Body Dopaminergic Neurons . . . . .	16
2.3.1 Multicolor Stochastic Labelling via FLP-out . . . . .	16
2.3.2 Fly Strains . . . . .	16

2.3.3	Immunohistochemistry . . . . .	17
2.3.4	Imaging . . . . .	18
2.3.5	Matching LM images with Seymour Data . . . . .	18
2.4	Loss-of-Function Behavioural Assays . . . . .	18
2.4.1	Fly strains . . . . .	18
2.4.2	Behavioural Experiments . . . . .	18
2.4.3	Behavioural Quantification . . . . .	19
2.4.4	Behavioural Data Analysis . . . . .	19
2.5	Ca <sup>2+</sup> Imaging with Light Sheet Microscopy . . . . .	19
2.5.1	Fly lines . . . . .	19
2.5.2	Sample Preparation . . . . .	19
2.5.3	LSM and Functional Imaging . . . . .	19
2.5.4	Data Analysis . . . . .	20
2.6	nomenclature . . . . .	20
<b>3</b>	<b>Results</b>	<b>21</b>
3.1	Strategy for identifying CX neuropils in the larval brain . . . . .	21
3.1.1	Identifying larva CX neuronal lineages . . . . .	22
3.1.2	Connectivity of CX neurons . . . . .	25
Sensory Inputs . . . . .	25	
Connectivity between CX Neuropils and Accessory Structures . . . . .	26	
3.2	The Central Complex of <i>Drosophila</i> Larva . . . . .	30
3.2.1	Protocerebral Bridge . . . . .	32
Larval PB Horizontal fibers . . . . .	32	
Larval PB Columnar neurons . . . . .	34	
PB Horizontal and PB Columnar connectivity . . . . .	35	
3.2.2	Ellipsoid Body . . . . .	36
Larval EB Wedge neurons . . . . .	36	
Larval EB Ring neurons . . . . .	37	
EB Ring Neurons and EB Wedge Neurons connectivity . . . . .	39	
3.2.3	Fan-Shaped Body . . . . .	39
Larval FB Tangential cells . . . . .	39	
Larval FB Columnar Neurons . . . . .	42	
Conectivity between FB Tangential and FB Columnar . . . . .	45	
Larval FB intrinsic neurons . . . . .	45	
3.2.4	Noduli . . . . .	46
3.3	Mushroom Body and the larval CX . . . . .	48

3.3.1	A loop between FB and the 'c' compartment of the MB . . . . .	48
3.3.2	Reciprocal connectivity between EB RNs and the 'g' compartment of the MB . . . . .	50
3.3.3	A loop between the NO and the MB vertical lobe via LAL . . . . .	50
3.3.4	The MB modulates inputs to the PB . . . . .	51
3.4	Visual Input into the larval CX . . . . .	52
3.4.1	VPNs inputs to the CX . . . . .	52
3.4.2	VLNs inputs to the CX . . . . .	55
3.5	Descending Neurons from CX . . . . .	57
3.6	Dopaminergic neurons (DANs) of the larval Central Complex . . . . .	59
3.6.1	8 pairs of DANs outside of the MB . . . . .	60
3.6.2	eDANs Connectivity . . . . .	62
3.7	Behavioural Assays - Loss of Function Analysis during green Light stimulation	64
3.8	Calcium Activity in response to Blue Light stimulation . . . . .	65
<b>4</b>	<b>Discussion</b>	<b>69</b>
4.1	Multisensory integration . . . . .	69
4.2	. . . . .	69
4.2.1	Navigation, place learning, and memory . . . . .	70
4.2.2	DANs in the FB and PB . . . . .	71
4.2.3	Conclusion . . . . .	72
<b>References</b>		<b>73</b>



# List of figures

3.1	Central Complex Neuron Classes . . . . .	27
3.2	Larval CX neuron boutons define the volumes of the 4 main CX neuropils .	29
3.3	The Central Complex Neuropils in Adult and Larva . . . . .	30
3.4	PB DALv1 Neurons . . . . .	33
3.5	PB columnar neurons . . . . .	34
3.6	<b>Ellipsoid Body Neurons.</b> Ring and Wedge Neurons with their corresponding lineages are shown. The mushroom body is coloured in magenta as a landmark in the larval brain. <b>A.</b> Ring neurons of lineage Dalv23, namely RN1/2a and RN1/2b; <b>B.</b> Ring neuron RN3 originating from lineage BAmv1/2; and <b>C.</b> The 8 EB wedge neurons (W1-8) originating from DALcl12 lineage. Panel <b>D.</b> depicts all these neurons stacked together to form the EB . . . . .	36
3.7	<b>EB Neurons Connectivity.</b> Both tables display the connectivity patterns among ring and wedge neurons in the ellipsoid body (EB). Each neuron is separated into left (_l) and right (_r) counterparts to represent lateralization. <b>Upper table:</b> axo-dendritic connections (color-coded in the green spectrum). <b>Lower table:</b> axo-axonic connections (color-coded in the yellow spectrum).	38
3.8	<b>FB tangential cells,</b> also known informally as "horseshoe" neurons for the shape of their bilateral axons. The seven hs-FB subtypes are shown, each with a morphological reconstruction (top) and a simplified schematic (bottom). Input synapses (dendrites) are indicated by blue arrows, and output synapses (axons) by red arrows. The mushroom body is shown in magenta. Neuron counts (left+right) are given below each schematic. <b>A–C.</b> Individual examples of hs-FB.1, hs-FB.2, and hs-FB.3. <b>D.</b> Overlay of hs-FB.1 through .3, illustrating the FB compartments they define. <b>E–H.</b> Individual examples of hs-FB.4 through .7. . . . .	41
3.9	FB Columnar Neurons . . . . .	43
3.10	Noduli Neurons . . . . .	47

3.11	Mushroom Body Connections to the Larval CX . . . . .	49
3.12	Visual Inputs via VPNs to larval Central Complex Neuropils . . . . .	54
3.13	Visual Inputs via VLNs to larval Central Complex Neuropils . . . . .	56
3.14	<b>Immunostained Dopaminergic Neurons of non-MB neurons.</b> Representative TH-GAL4 flp-out labelled neurons in the Drosophila larval brain classified as central-complex dopaminergic neurons (eDANs). Three secondary antibodies were used, but only the channel showing the neuron of interest is displayed in each panel; the neuron signal is rendered green for consistency and background staining is tinted purple to improve contrast. Arrows mark the soma of the neuron of interest from a specific channel. On the right side of each confocal image, the EM 3D reconstruction of the corresponding neuron is shown. . . . .	61
3.15	eDANs Connections to the CX . . . . .	63
3.16	Loss of Function Analysis during Light Stimulation . . . . .	64
3.17	Lightsheet volume Segmentation . . . . .	66
3.18	Neural Activity of the Larval Brain in response to Photoreceptors Rh5 Stimulation . . . . .	67

# List of tables

1.1	Major Connectomic Datasets . . . . .	2
1.2	<i>Drosophila</i> Adult Central Complex Lineags . . . . .	13
1.3	<i>Drosophila</i> Adult Central Complex Neurons . . . . .	14
3.1	Lineages of the Adult CX that also contribute neurons to the Larval CX . . . . .	23
3.2	Larval Central Complex Lineages . . . . .	24
3.3	Contribution of lineages to CX . . . . .	25
3.4	Monosynaptic connectivity between CX neuropils . . . . .	28
3.5	CX Core Neurons . . . . .	28
3.6	The Neurons of <i>Drosophila Larva Central Complex</i> . . . . .	31
3.7	PB Horizontal Neurons connection to PB columnar . . . . .	35
3.8	Connectivity between FB Tangential and FB Columnar neurons. Cell shading corresponds to relative connection strength (darker = stronger). . . . .	46
3.9	Summary of NO.d neurons . . . . .	48
3.10	CX Descending Neurons . . . . .	58
3.11	Behaviour of CX Descending Neurons . . . . .	59
3.12	<b>Neurons tested for LOF</b> Neuron names, corresponding split GAL4 line used for LOF experiments, and lineage information. . . . .	65



# Chapter 1

## Introduction

### 1.1 Mapping brains - The Power of Connectomics

Investigating the origins of human behaviour and mapping it to onto the brain is a mission as old natural philosophy. Hippocrates was the first to identify the brain as the 'analyst of the outside world', the interpreter of consciousness and the center of intelligence and willpower (Breitenfeld et al., 2014), and to this day he is considered the forefather of neurology.

At its heart, neuroscience has always been about reverse engineering human behaviour. We attempt to understand the full functionality of the brain from its underlying anatomical features - molecular and cellular - its activity and its circuits. Ultimately, the goal is to infer causality about behaviour using the best tools we have at our disposal (McKinstry-Wu & Kelz, 2013).

Detailed maps of synaptic connectivity (also known as wiring diagrams) are a core to our understanding of the fundamental link between brain and behaviour and, crucially, how malfunctions of it can result in behavioral or neurological disorders. Whilst large-scale circuit reconstructions aren't yet possible with state-of-the-art imaging technology - the human brain has 86 billion cells Herculano-Houzel, 2009, with tens of thousands of synapses each, and would take centuries to map - advances in tiny brains mapping are pushing the brain sciences by unraveling causal and correlative relations between structure and function and paving the way to establishing fundamental principles of how neural systems operate.

Connectomics - the study of complete sets of connections in individual neural systems - is at large responsible for a lot of these advancements. It allowed us to create roadmaps for brain of various animals such as the *C. Elegans* - the first landmark study of a connectome (Brenner, 1974) -, the mouse visual cortex ("Functional connectomics spanning multiple areas of mouse visual cortex", 2025), the *Drosophila* adult (Scheffer et al., 2020) as well as the *Drosophila* larva (Berck et al., 2016; Eichler et al., 2017; Eschbach et al., 2021, 2020;

Organism	Tissue / region	Neurons	Imaging method	Project / Reference
<i>C. elegans</i>	Entire CNS	302	ssTEM	White et al. (1986); Witvliet et al. (2021, <i>Nature</i> )
<i>C. intestinalis</i> (larva)	Entire CNS	177	ssTEM	Ryan et al. (2016, <i>eLife</i> 16962)
<i>P. dumerilii</i> (larva)	Entire CNS	9 162	ssTEM	Veraszto et al. (2024, <i>eLife</i> 97964)
<i>D. melanogaster</i> (larva)	Entire CNS	~9 700	ssTEM	Winding et al. (2023, <i>Science</i> )
<i>D. melanogaster</i> (adult)	Entire brain	~135 000	ssTEM	Zheng et al. (2018, <i>eLife</i> 16962; <i>Cell</i> )
<i>M. musculus</i>	Visual cortex (VISp + HVAs)	~100 M (per mm <sup>3</sup> )	SBF/MB-EM	MICRONS v3 ( <i>Nature</i> , 2025)

**Table 1.1 Fully-mapped Connectomic Datasets** Comparison of major connectomic datasets across species, from *C. elegans* to mouse visual cortex. All values are directly reported in the cited publications; no extrapolated voxel or volume data are included. Abbreviations: ssTEM, serial-section transmission EM; SBF/MB-EM, serial block-face or multi-beam EM.

Larderet et al., 2017; Ohyama et al., 2015). All these datasets were obtained via a technique known as electron microscopy (EM, ssEM, TEM, FIB-SEM) and have become foundational references in neuroscience, ushering in the long-anticipated era of synaptic wiring diagrams (Table 1.1).

EM is, to this day, the highest-resolution technology for brain mapping, allowing us to visualize the smallest neurites (as small as 15 nm; (Meinertzhagen, 2016)) and all the synaptic connections—vesicles and clefts (40 nm and 20 nm, respectively)—between them. The great advantage of tiny animal models such as *Drosophila* is that their physical dimensions ( 600  $\mu\text{m}$  or 0.15  $\text{mm}^3$  for the adult fly brain; 242  $\mu\text{m}$  or 0.001  $\text{mm}^3$  for the larval nervous system) can be reconstructed with synaptic resolution within a manageable timeframe and cost. Their dimensions - no neuropil greatly exceeds 50  $\mu\text{m}$  in depth (Meinertzhagen, 2016) — also facilitate the use of multimodal imaging approaches: confocal microscopy for molecular and genetic labeling, light-sheet microscopy for rapid volumetric imaging (sometimes paired with calcium activity), and electron microscopy for ultrastructural detail—on the same specimen or across comparable samples.

The female adult vinegar fly *Drosophila Melanogaster* is one of the largest pieces of nervous tissue collected and imaged by EM (i.e., FAFB; (Zheng et al., 2018)). The dataset encompasses 40 teravoxels and 21 million serial section transmission EM images, covering a  $995 \times 537 \times 283 \mu\text{m}$  volume at  $4 \times 4 \times 40 \text{ nm}$  resolution. Complementary to this, a complete EM reconstruction of the *Drosophila* larva central nervous system ((Winding et al., 2023)) spans the entire brain and ventral nerve cord within a roughly 242  $\mu\text{m}$  volume, capturing approximately 9,700 neurons at  $3.8 \times 3.8 \times 50 \text{ nm}$  resolution. I have contributed to mapping the larval fruit fly, specifically, in unraveling a new area responsible for navigational decisions. This area is known as the Central Complex in the adult, and, as I will go on to show, I postulate that an analogous, numerically smaller Central Complex exists at the larval stage of development.

Together, these datasets bridge developmental stages of the fly nervous system, enabling both sparse and dense connectomic analyses that inform a growing range of hypotheses around their relevance to function and behaviour. Collectively, connectomic datasets provide a structural framework through which brain function can be interpreted. They transform anatomy into networks and reveal not only which neurons are connected but also the direction of information flow. This is the exact type of data that is translatable into connectivity matrices — quantitative maps of presynaptic and postsynaptic partnerships— that we can therefore use we can infer circuit logic and predict functional pathways to expose hidden motifs, highlight convergence or divergence across modalities, and delineates subnetworks anatomical areas that underlie specific behaviours. Using *Drosophila* is powerful approach to functionally study these detailed wiring diagram, because it is one of the most experimentally accessible animal model.

## 1.2 The advantage of the *Drosophila* larva brain

Historically, for connectomes of larger insects of vertebrates, connectomes of isolated areas have been studied and made sense of. However, brain regions don't operate in isolation and connectivity inside the whole brain spans multiple dispersed areas, neurons can converge or diverge towards each other, and understanding any single computation requires understanding its inputs, outputs and relation to other regions of the brain (Huang et al., 2020). Functional (Ca activity) studies confirm this to be the case in *Drosophila* (Lemon et al., 2015)as well as in vertebrates (Ahrens et al., 2013).

A smaller circuit is therefore advantageous for its accessibility to assess dispersed neural computations. With its nervous system comprising 12 000 neurons and only 2,500 of these inside the brain - all of which have been mapped with synaptic resolution using whole-CNS EM, and its brain networks mostly reconstructed - the fruit fly larva is especially well suited for brain-wide circuit studies. This animal's circuit architecture is stable across larval stages (1st, 2nd and 3rd instar) with neurons only growing in size but not changing synaptic partners (Gerhard et al., 2017). In addition, the larva vinegar fly has rich but numerically limited adaptive behaviour that is equivalent from 1st to 3rd instar (Almeida-Carvalho et al., 2017).This means that behaviour observed in later stages(which can be a favourable choice as they are more easily identified by cameras and generally easier to work with ) can be mapped onto our circuits from the 1st instar.. Brain structures homologous to adult and other insect species ((Carreira-Rosario et al., 2018; Eichler et al., 2017; Truman et al., 2023))

Not only does the larval fly have a full synaptic-resolution connectome, this animal has a vast library of genetic driver lines (GAL4, LexA) for targeted gene expression in individual

neurons, as well as effector line (UAS, LexOp), which allows for controlled expression of proteins that allow (e.g.) optogenetic manipulation via CsChrimson (Kim et al., 2015) or monitoring neural activity via GCaMP7 (Owald et al., 2015).

Our ability to genetically manipulate protein expression in individual neurons and record their activity in freely behaving larvae, as well as quantify simple output behaviours (Vogelstein et al., 2014), link them directly to their circuit and infer from adult structures, makes it a very tractable option to identify specialised, functionally distinct natural networks from our reconstructed larval circuits.

### 1.3 Navigation: Fundamental Across Species

When one wants to inspect connectivity maps to understand universal principles of neural computations, one must start with the fundamentals and ask themselves: what are some aspects of the brain that are universally true across species?

Certainly what is true for all species is they need to find resources, shelter and avoid threats by navigating their environment. Navigation is therefore a fundamental and crucial function of biological systems across the board.

Navigation is achieved via multisensory integration, a process wherein sensory cues are integrated into one coherent neural representation, to maximize sensitivity and reduce ambiguity. Interpreting sensory inputs requires dynamic transformations that allow the brain to ignore transient sensory distractions and compensate for fluctuation in the quality of information or its temporal availability. Once sensory inputs are processed, they're followed by action selection via activation of specific muscles.

During navigation, the brain is able to retain a model of the world (i.e. neural representations of the external world persist) in absence of sensory input. This relies on attractor dynamics generated by referral neural circuits in the deep brain regions rather than at the sensory/motor periphery.

Deep-brain circuits' inputs and outputs are usually difficult to identify and characterize, especially those involved in flexible navigation whose circuits have large populations of neurons. Importantly, deep-layer connectivity is nearly impossible to determine in large brain animals, such as mammals. For this reason, smaller animals, such as insects are best suited for such studies, with their numerically smaller, tractable neural circuits, they provide the opportunity to obtain a detailed understanding of deep-layer computations underlying navigation.

Insects are expert navigators. They maintain a specific pattern of action selection over many minutes and even hours during behaviors like foraging or migration, and maintain a

prolonged state of inaction during quiet wakefulness or sleep (Hendricks et al., 2000; Shaw et al., 2000). These behaviors are initiated and modulated based on environmental conditions (for example, humidity, heat, and the availability of food, nutritive state, hunger, hydration etc) and an insect's internal needs (such as sleep drive and nutritive state; Griffith, 2013). The context-dependent initiation and control of many such behaviors has been shown to depend on a conserved insect brain region called the central complex (also known as CX)

## 1.4 The Central Complex

*Parts of this section incorporate text from published work [The central complex of the larval fruit fly brain] (Lungu et al., 2025)*

### 1.4.1 Central Complex across insects

The Central Complex (CX) is a conserved set of neuropils found across arthropods (bumblebee, the red flour beetle, Monarch butterfly) that acts as a sensory integration area and a center for coordinated motor activity (Heinze, 2024; Pfeiffer & Homberg, 2014; Turner-Evans & Jayaraman, 2016).

Ancestrally, the central complex arises during embryogenesis in hemimetabolous insects - insects that undergo ‘incomplete’ metamorphosis, whose nymph stages transition slowly over multiple steps into the adult shape, with their brain developing gradually(e.g. beetle or cicada). Later derived holometabolous insects - those that compress all nymph stages into a sessile stage(the pupa) - undergo ‘complete metamorphosis’, and have distinct larval, pupal and adult stages designed to restrict developmental resources to those needed for growth. In this case, the central complex arises during postembryonic stages (e.g. flies, moths, bee).

This brain region originated more than 400 million years ago and has remained highly conserved across insect species, comprising 4 neuropils: the protocerebral bridge (PB), the ellipsoid body (EB; or central body lower unit/CBL), the fan-shaped body (FB; or central body upper unit), and a pair of noduli (NO). The CX is known for its stereotypical regular neuroarchitecture composed of vertical columns(columnar neurons) and horizontal layers (tangential neurons). Columnar neurons link the PB with the other CX neuropils (EB,FB,NO) forming columnar compartments in each of them. Tangential cells input horizontally across the entire surface of a neuropil, and intersect with columnar neurons (Honkanen et al., 2019).

### 1.4.2 Central Complex of Adult *Drosophila*

In the fruit fly, the central complex starts forming during late larval and metamorphic stages, via the proliferation of pioneer undifferentiated neurons that remain quiescent until the pupal stage. This is in contrast to other holometabolous insects such as the tribolium (Farnworth et al., 2022) whose CX cells begin arborizing during embryogenesis.

In *Drosophila melanogaster*, the functions of the CX include multi-sensory navigation, path integration, place learning, allocentric orientation of the head relative to its body, sleep regulation, and providing an internal sense of direction in the absence of stimuli, among others (Fisher, 2022; Franconville et al., 2018; Hanesch et al., 1989; Heinze et al., 2018; Ofstad et al., 2011; Pfeiffer & Homberg, 2014; Pisokas et al., 2020; Seelig & Jayaraman, 2013; Shafer & Keene, 2021; Stone et al., 2017; Szuperak et al., 2018).

At the adult stage, the fruit fly CX has four well-studied neuropils: the Protocerebral Bridge (PB), the Fan-shaped Body (FB), the Ellipsoid body (EB) and the Noduli (NO) (Hanesch et al., 1989) plus, as of recently, the Asymmetrical Body (AB) (Wolff & Rubin, 2018), in addition to several smaller accessory neuropils often referred to as the lateral complex: the gall (GA), the lateral accessory lobe (LAL) - which is interconnected with all other neuropils - and the bulbs (BU) (Franconville et al., 2018; Hulse et al., 2021; Wolff et al., 2015).

The Central Complex neuropils originate primarily from DM lineages (DM1-DM6) in addition to neuropil specific ones (Table 1.2) (Andrade et al., 2019; Yang et al., 2013). The DM1–DM4 lineages generate the small-field columnar neurons that innervate all the four major CX neuropil (PB, FB, EB, NO) in highly ordered isomorphic patterns to establish projections across different CX compartments. Other lineages are more specialised, such as DM5 which exclusively innervates the PB, or DL1 which only innervates the FB.

#### Protocerebral Bridge (PB)

In the adult *Drosophila*, the PB comprises two sets of bilaterally symmetric compartments, sometimes referred to as glomeruli 1–9 Hulse et al., 2021, positioned at the most posterior-dorsal location possible in the brain.

These compartments are arranged in a continuous manner medio-laterally, contacting at the midline. In the adult, about 600 neurons innervate the PB, organized into hundreds of types ( 194 (Wolff et al., 2015), see Table 1.3) that are split into two main general groups: the columnar neurons (from lineages DM1, DM2, DM3, DM4 and DM6) whose dendrites innervate one or more of the 9 + 9 compartments of the PB (Wolff et al., 2015); and the

horizontal neurons (also known as horizontal fibers) derived from a single lineage (PBp1; (Andrade et al., 2019)) whose axons innervate many or all PB compartments.

In the adult, the PB receives visual input via relay neurons (POL neurons) conveying information on polarized light, in a highly structured pattern across its compartments that binarizes the continuum of angles of polarized light ((Heinze et al., 2009)). Then the PB relays this information to the EB compartments (Fig.).

In addition to visual input, the adult PB also integrates olfactory inputs (Hulse et al., 2021), suggesting that spatial navigation is not unimodal but integrative across multiple sensory modalities.

### **Ellipsoid Body (EB)**

The adult Ellipsoid Body (EB) is a ring-shaped structure situated between the Fan-Shaped Body (FB) and the Mushroom Body horizontal lobes, facing anterodorsally. The EB is made of two main types of neurons: Ring-neurons (ERs; derived mainly from the EBAa1/DALv2 and LALv1/BAmv1/2 lineages) that spread their axons across the length of the EB, and reciprocally connected Wedge neurons (EPGs, derived from the DM4 lineage) that divide the EB into 16 compartments (the wedges) (Wolff et al., 2015). The EPG (Wedge) neurons are excitatory and synapse with each other, as well as reciprocally with the Ring neurons, which are inhibitory (Franconville et al., 2018; Hulse et al., 2021).

The adult EB circuit has been modeled as a ring attractor (Stone et al., 2017) to, in concordance with its anatomy, reproduce *in silico* the observed "bump" of neural activity in the form of a sole active wedge in the *Drosophila* adult EB (Seelig & Jayaraman, 2015).

EPG (Wedge) neurons form 16 wedges around this ring, and project to both hemispheres of the PB, where they connect to two sets of columnar neurons (PEG and PEN) that project back to the EB, forming recurrent loops. The anatomical offset between EPG and PEN neurons is key to how the fly head direction system translates angular motion into an updated position of the activity bump in the ring attractor (Stone et al., 2017).

In the adult, the EB receives visual inhibitory GABAergic inputs, via two parallel pathways for distinct visual information: 1. Ring neurons that map the visual environment of the fly; 2. tangential neurons that take in information about body rotations and translational velocity. The latter receive input in the LAL and output to the NO.

Mechanosensory input also enters the CX via the second-order projection neurons to the EB. These neurons code head direction; some proprioceptive input has also been observed (Hulse et al., 2021). It receives strong inputs from PB, NO and the LAL, and outputs onto the PB.

### Fan-Shaped Body (FB)

The adult FB is a bilaterally symmetric neuropil posterior and dorsal to the EB, with well-defined horizontal and vertical components: 6 horizontal layers stacked dorso-ventrally that are defined by distinct sets of horizontal neurons (FB tangential neurons); and 9 vertical columns stacked medio-laterally are defined by column-specific columnar neurons. Both horizontal and vertical neurons innervate the FB in a layer- and column-restricted manner (Heinze, 2017). As the biggest CX neuropils, a large variety of lineages contribute to the FB (see Table ??). In the adult FB there are 2 types of FB tangential cells: (1) neurons that relay the presence of an attractive odor to the FB, originating in the MB or the LH (learnt or innate valences; (Hulse et al., 2021)); (2) neurons that relay sleep drive to the FB, whose activity is mandatory for sleep initiation (Shafer & Keene, 2021).

The adult FB columnar neurons, or columnar input cells, are known as PFN (PB-FB-NO; (Wolff & Rubin, 2018)), with dendrites in the PB and axonic outputs on both the FB and NO. There are 5 main types (Hulse et al., 2021), with their arbors tiling the PB glomeruli, the FB layers, and the NO layers.

The third class of adult FB cells are interneurons with dendrites and axons within the FB. Of these there are 2 main types: FB intrinsic neurons whose arbors lay entirely within the FB, and FB mixed arborisation neurons with additional axonic branches outside the CX and sometimes dendritic branches in the PB (Wolff et al., 2015).

A key feature of the the adult FB is strong innervation by MB Output Neurons (MBONs) (Hulse et al., 2021; Scheffer et al., 2020). In addition, the axons of dopaminergic neurons driven by visual inputs innervate the FB (Lin et al., 2013).

### Noduli (NO)

The noduli are small, bilaterally symmetric spherical neuropils located medially and ventrally to the FB. In the adult *Drosophila* brain, each hemilateral neuropil is divided in 3 subunits: nodulus 1, 2 and 3 (NO1, NO2, NO3), with NO1 having the highest synaptic density of the three. There are notable variations across insect species, with the number of noduli ranging from two to four per brain hemisphere. While the stacked noduli subunits have been referred to as horizontal layers, no vertical subdivisions have been reported for these structures. Therefore no columnar organization is known.

The NO neurons present a unique morphology featuring compact, clutched axons, which set them apart from other CX neurons (Hulse et al., 2021; Wolff & Rubin, 2018) and greatly ease their identification even in the absence of the typical conspicuous anatomical neuropil

region present in adult insects. In the adult fruit fly, these neurons primarily originate in the DM1, DM2 and DM3 lineages (Andrade et al., 2019).

In the adult *Drosophila* brain, the NO is interconnected with the EB and the FB, with the latter relaying information to the NO from tangential input neurons via several PB columnar cells such as PEN-neurons (PB-EB-NO; from the head direction system) and PFN-neurons (PB-FB-NO) (Hulse et al., 2021; Wolff et al., 2015). The primary NO inputs outside of the CX are from the LAL; these are known as LNO neurons and are suggested to be inhibitory (Hulse et al., 2021; Wolff & Rubin, 2018). LNOs send inputs to and receive feedback from columnar neurons. FB tangential neurons make weak reciprocal connections to LNOs and columnar neurons in the NO. All columnar neurons (PFNs and PENs) that synapse onto NO (are NO.b) are recurrently connected to the same LNO (LAL-NO) neurons they receive input from.

### **Neuromodulatory neurons in the CX**

In the adult CX numerous neurons express neuromodulators and neuropeptides, and their receptors, particularly in the FB (Kahsai & Winther, 2011; Kahsai et al., 2012). These modulatory molecules have been associated with the overall level of motor activity and the regulation of sleep (Donlea, 2019), among other roles (Pfeiffer & Homberg, 2014). Here, we list the subset of neurons with assigned neuromodulators that are monosynaptically connected to CX neurons in the larval brain.

The sVUM2mx and sVUM2md are a pair of octopaminergic ventral unpaired medial (VUM) neurons with somas in the SEZ and bilaterally symmetric arbors, which innervate the larval optic neuropil (LON; (Larderet et al., 2017)). These octopaminergic neurons further project their axons into the LAL and also deliver axonic boutons to the EB.

Another octopaminergic VUM (a ladder neuron), named MB2IN-191 (Eschbach et al., 2020), innervates the FB bilaterally but not exclusively, with its bilateral axon extending further into nearby medial and posterior areas of the brain.

Given the known role of octopamine in controlling sleep/wake in larvae (Szuperak et al., 2018) and the role of the adult CX in modulating motor activity levels and sleep (Pfeiffer & Homberg, 2014; Shafer & Keene, 2021), these octopaminergic neurons should be tested experimentally for their potential in mediating a signal for sleep in larvae.

Furthermore, the pair of SP2-1 serotonergic neurons described for the optic lobes (Larderet et al., 2017) present ipsilateral dendrites that integrate inputs from multiple PB.b neurons and also FB.b (hs-FB.6), and then project their axons contralaterally, extending across the PB and into the optic lobe, dropping presynaptic connections onto PB.d neurons and then further posterior and lateral until reaching the LON. These neurons are ideally suited

for relaying feedback signals onto the optic lobe to modulate the processing of incoming visual inputs as a function of PB and FB activity.

Another serotonergic neuron, CSD (Berck et al., 2016), that integrates inputs from olfactory sensory neurons (ORNs) and the superior lateral protocerebrum (an extended area around the LH), and projects back to the antennal lobe (AL) to modulate olfactory LN function (Vogt et al., 2021), integrates strong inputs from the FB intrinsic neuron MB2ON-125.

Taken together, via SP2-1 and CSD neurons the output of the FB may modulate with serotonin both the LON and the AL, presumably to provide context to first-order circuits for sensory processing (vision and olfaction), as has been reported for hunger versus satiation (Vogt et al., 2021).

### Mushroom Body and the CX

In the adult **Drosophila**, the Mushroom Body is known to output onto the Central Complex neuropils through the MB Output Neurons (MBONs). At this stage, adult MBONs primarily target the Fan-shaped Body - tangential neurons from the middle layers (4-6) - and the Noduli - via a direct glutamatergic connection from MBON-30 to LCNOp(LAL-NO) neurons which then target the PFN (PB-FB-NO) neurons (Hulse et al., 2021).

## 1.5 Larval Central Complex as a research opportunity

What is special about the holometabolous insects such as *Drosophila* is the extremely arrested brain development during larval stages (Andrade et al., 2019). This suggests that other larval neurons must take over essential navigational functions performed by the adult central complex, in the form of what we expect to be an earlier stage larval central complex.

In *Drosophila melanogaster*, the functions of the CX include multi-sensory navigation, path integration, place learning, allocentric orientation of the head relative to its body, sleep regulation, and providing an internal sense of direction in the absence of stimuli, among others (Fisher, 2022; Franconville et al., 2018; Hanesch et al., 1989; Heinze et al., 2018; Ofstad et al., 2011; Pfeiffer & Homberg, 2014; Pisokas et al., 2020; Seelig & Jayaraman, 2013; Shafer & Keene, 2021; Stone et al., 2017; Szuperak et al., 2018).

The fruit fly larva exhibits a range of behaviors that require spatial navigation, including chemotaxis for foraging and escape (Davies et al., 2015; Ebrahim et al., 2015; Fishilevich et al., 2005; Khurana & Siddiqi, 2013) and aversive phototaxis in response to blue light (Gong, 2009; Keene & Sprecher, 2012; Sawin-McCormack et al., 1995). In addition to responding to an isolated unimodal stimulus, the larva integrates competing stimuli prior to

decision making for navigation (Gepner et al., 2015). Furthermore, larvae sleep, which is required for long-term memory (Poe et al., 2023) just like in the adult fly (Donlea, 2019; Donlea et al., 2011), where sleep is regulated by the central complex (Shafer & Keene, 2021).

Anatomically, the larval central brain shares the set of neuroblasts with the adult (Lacin & Truman, 2016), and presents neuropil areas that directly correspond to those of the adult brain such as the Antennal Lobe (AL), the Mushroom Body (MB), and the Lateral Accessory Lobe (LAL), in addition to more larval-specific neuropils such as the larval optic neuropil (LON) (Pereanu et al., 2010). The organization and synaptic connectivity of the larval AL, MB, and LON are well understood at present (Berck et al., 2016; Eichler et al., 2017; Larderet et al., 2017).

Nevertheless, these neuropils constitute only ~30% of the complete larval brain connectome by number of neurons (Winding et al., 2023). We postulate that amongst the remaining ~70% of brain neurons, and given the reported conservation of neuroblasts (Lacin & Truman, 2016) and neuronal identities from larval to adult (Truman et al., 2023), and the larval behaviors in navigation and sleep that in the adult are associated with the CX, the question of whether the larval brain harbors a simpler yet homologous set of Central Complex neuropils must be examined. Furthermore, in other holometabolous insect orders, neuroblast proliferation arrests at a later point in the stereotyped sequence of neuron types (Truman & Riddiford, 1999), generating more neurons embryonically and rendering the central complex identifiable at the larval stage, such as in the beetle *Tribolium castaneum* where the CX develops embryonically (Farnworth et al., 2020; Koniszewski et al., 2016). In the fruit fly larva, hundreds of late embryonic-born neurons known to later on pioneer the development of the adult CX remain undifferentiated throughout larval life (Andrade et al., 2019).

The larval brain, though, does not present fused brain hemispheres like in the adult. With adult CX neuropils being largely medial structures, any putative larval brain counterparts will differ significantly by morphology alone. The basis of our search for the larval CX has to rely on (1) neuronal lineages generated by the same neuroblasts; (2) the relative spatial location of neurons within the overall neuropil since these are conserved for neuropils known to be homologous such as the AL, MB, LON and LAL; (3) the synaptic circuit architecture organizing the adult central complex neuropils; and (4) the patterns of sensory inputs. For (1) we use embryonic-born neurons that remain identifiable yet undifferentiated throughout larval life, a subset of which will develop into the adult CX (Andrade et al., 2019). For (2), (3) and (4) we rely on the fully reconstructed neuronal arbors constituent of the complete connectome of the larval brain (Winding et al., 2023), together with prior publications on larval sensory systems (Berck et al., 2016; Hernandez-Nunez et al., 2021; Hückesfeld et al., 2021; Larderet et al., 2017; Mast et al., 2014; Mirochnikow et al., 2018; Ohyama et al.,

2015; Schlegel et al., 2016). We use all four in an iterative process to progressively discover the complete list of neurons composing the putative larval CX.

This thesis aims to identify the putative central complex neuropils of the *Drosophila* larva, characterize their connectivity pathways, neurotransmitter identity, and functional role in behavior, and place these findings in the context of central complex evolution and developmental diversity. To achieve this, I combined connectomic reconstructions, genetic tools, functional imaging, and behavioral assays. The thesis is structured as follows: Chapter 2 describes the analytical and experimental methods used across the study, Chapter 3 presents the main results in the context of specific research questions, and Chapter 4 discusses the implications of these results for our understanding the structure and function of a central complex at an earlier developmental stage of a holometabolous insect.

Neuropil	Lineage
<b>Protocerebral Bridge</b>	DM1 (DPMm1) DM2 (DPMpm1) DM3 (DPMpm2) DM4 (CM4) DM5 (CM5) DM6 (CM3) PBp1 (-)
<b>Ellipsoid Body</b>	DM1 (DPMm1) DM2 (DPMpm1) DM3 (DPMpm2) DM4 (CM4) DM6 (CM3) EBa1 (DALv2) LALv1 (BAMv1)
<b>Fan-Shaped Body</b>	DM1 (DPMm1) DM2 (DPMpm1) DM3 (DPMpm2) DM4 (CM4) DM6 (CM3) DL1 (CP2) EBa1 (DALv2) LALv1 (BAMv1) AOTUv4 CREa1 (BAMd1) CREa2 (DALCm1) SMPad2 (DAMd2/3) SIPp1 (DPMpl2)
<b>Noduli</b>	DM1 (DPMm1) DM2 (DPMpm1) DM3 (DPMpm2) DM4 (CM4) LALv1 (BAMv1) DM6 (CM6) SAMPad2 (DAMd2/3)

Table 1.2 *Drosophila* Adult Central Complex Lineags. Individual Central Complex neuropils and their contributing lineages in the nomenclature of ItoLee(Lai et al., 2008) and (Hertenstein)(Lovick et al., 2013)

Hulse et al Name	Wolff/Francoville Name
<b>EB</b>	
<i>Ring Neurons</i>	
ER 1–6	BU.s EB.b
<i>Extrinsic Ring Neurons</i>	
ExR1–8 (Extrinsic Ring)	NO/BU/LAL/GA.s EB.b
<i>Wedge Neurons</i>	
EPGt (EB–PB Columnar)	EB.s PB.b GA-t.b
EPG (EB–PB Columnar)	EB.s PB.b GA.b
EL (EB Columnar)	EB.s GAs.s.b
WL–L	Wedge–LAL.s.b
<b>PB</b>	
PEN (EB–PB Columnar)	PB.s EB.b NO.b
PEG (EB–PB Columnar)	PB.s EB.b GA.b
PFN (PB–FB Columnar)	PB.s FB.b NO.b
PFR (PB–FB Columnar)	PB.s FBd.b ROB.b
PFG (PB–FB Columnar)	PB.s FB.s.b GA.b
PFL1–3 (PB–FB Output)	PB.s FB.s LAL.b CRE.b
Delta 7 (PB Intrinsic)	PB.s.b
P–ECG	PB.s EB.b GA.b
P1–9 (Octopaminergic)	PB.s EB.b GA.b
LPsP (Dopaminergic)	PB.b LAL.s PS.s
Sps–P	PB.b SPS.s
IbSpsP	PB.b IB.s.SPS.s
P6–8P9 (intrinsic)	PB.s.b
<b>FB</b>	
vDelta (Intra–FB Columnar)	FB.s.b
hDelta (Intra–FB Columnar)	FB.s.b
FR (FX Columnar)	FB.s ROB.b
FS (FX Columnar)	FB.s SNP.b
FC (FX Columnar)	FB.s CRE.b
FB Tangential (FBt)	FB.s (..)
<b>NO</b>	
LNO–1 (LG–N/GLNO)	LAL.s GA.s NO.b
LNO–2 (LNA)	LAL.s NO.b
LNO–3 (LCNOp/LCNOp)	LAL.s CRE.s NO.b

Table 1.3 *Drosophila* Adult Central Complex Neurons This table contains CX neurons nomenclature according to Hulse et.al (Hulse et al., 2021) mapped onto Wolff et al(Wolff & Rubin, 2018) and Francoville (Franconville et al., 2018) nomenclatures which contain information about the location of input regions (.s for dendritic spines) and output regions (.b for axonal boutons)

# Chapter 2

## Methods

*Parts of this section incorporate text from published work [The central complex of the larval fruit fly brain] (Lungu et al., 2025)*

### 2.1 Reconstructing neurons in Electron Microscopy Volumes

#### 2.1.1 Connectome data

The connectome of a 2-hour old first instar larval brain was used, as reconstructed previously by us (Winding et al., 2023). The neuronal reconstructions, synapse labels, and neuron annotations, together with the electron microscopy volume, is available at the VirtualFlyBrain

#### 2.1.2 Neurons Segmentation

Neurons were manually segmented using CATMAID

#### 2.1.3 Data Analysis

Data was analysed via the web-based CATMAID software (Saalfeld et al., 2009; Schneider-Mizell et al., 2016), specifically

Results were exported as readable tables mapping neuropil-level connectivity and graph measures. For each neuropil we report: total incoming synapses, total outgoing synapses, in-/out-strength, degree, betweenness, eigenvector centrality, clustering coefficient, and assigned community. Tabular outputs were produced as CSV and as LaTeX tables for inclusion in the

manuscript and Supplementary Materials. Code and raw matrices used to generate the tables are provided in the project repository to ensure reproducibility.

## 2.2 Identification of Central Complex Neuropils

## 2.3 Identifying non-Mushroom Body Dopaminergic Neurons

### 2.3.1 Multicolor Stochastic Labelling via FLP-out

We were interested if any of the identified central complex neurons are dopaminergic. To verify that, we used the GAL4/UAS system to tag all the dopaminergic neurons(DANs) in the brain, and focused on those located outside the Mushroom Body (non-MB DANs).

We used the MCFO approach to label dopaminergic neurons inside the brain of *drosophila* larva. To do this we used the TH-GAL4 driver line, which expresses GAL4 in dopaminergic neurons. The GAL4 gene is inserted under the control of the tyrosine hydroxylase (TH) promoter, which is specific to DANs, so it's expressed in TH+ (dopaminergic) neurons.

To achieve stochastic multicolor labeling of individual neurons, we used the Multicolor FlpOut (MCFO) system, which relies on FLP recombinase-mediated excision of FRT-flanked transcriptional stop cassettes placed upstream of multiple fluorescent reporter genes. FLP recombinase expression was driven under UAS control and activated by tissue-specific GAL4 drivers. Upon FLP expression, recombination at FRT sites excises stop cassettes in a random subset of cells, allowing expression of distinct fluorescent proteins from a single transgenic construct. This results in combinatorial multicolor labeling of individual cells, enabling detailed morphological analysis. Our line had three MCFO reporters(smGFPs) HA, FLAG, V5.

### 2.3.2 Fly Strains

We used TH-GAL4, a line that tags all dopaminergic neurons in the central nervous system of the larva (Selcho et al., 2009), and crossed it with tsh-GAL80 to suppress expression in the VNC. The following driver line was used: R57C10-FlpL in su(Hw)attP8;; pJFRC210-10XUAS-FRT>STOP>FRT-myR::smGFP-OLLAS in attP2. pJFRC210-10XUAS-FRT>STOP>FRT.... The following effector line was used: w; tsh-Gal80/cyo.Tb.RFP; TH-Gal4. These were crossed, and the desired progeny was: R57C10-FlpL / + ; tsh-Gal80 / CyO.Tb.RFP ; TH-Gal4 / UAS-smGFP. To select for larvae that express GAL4 only in the

brain, only larvae with red fluorescent bodies were dissected, as this indicates the presence of tsh-GAL80.

### 2.3.3 Immunohistochemistry

For Immunohistochemistry, we adapted the protocol from HHMI Janelia Research Campus, in combination with the protocol from (Nern et al., 2015). The following primary antibodies were used: **Mouse  $\alpha$ -Neuroglan; Rabbit  $\alpha$ -HA Tag; Rat  $\alpha$ -FLAG Tag** (Sigma). The following secondary antibodies were used: AF488 Donkey  $\alpha$ -Mouse; **DL549 Goat  $\alpha$ -Rabbit (Sigma)**. The following conjugated antibody was used: AF647 Mouse  $\alpha$ -V5

Optimization of the protocol required extensive iteration over many months, during which multiple combinations of primary, secondary, and conjugated antibodies were systematically tested. The aim was to obtain strong, specific signals in all imaging channels without cross-reactivity or bleed-through. The final antibody set reported here represents the outcome of this process and was selected because it consistently provided clear labeling across epitopes, enabling reliable multichannel visualization.

The larval central nervous system (CNS) was dissected in cold 1× phosphate-buffered saline (PBS). The tissue was then transferred into 2 mL Protein LoBind tubes containing cold 4% paraformaldehyde (PFA) in 1× PBS, and incubated for 1 h at room temperature (RT) while nutating. The PFA was then removed and tissues were washed in 1.75 mL of 1% PBT (PBS with 0.3% Triton X-100) four times for 15 min each with nutation. Samples were then blocked with 5% Normal Donkey Serum (NDS Jackson Immuno Research; prepared as 95  $\mu$ L PBT + 5  $\mu$ L NDS), and incubated for 2 h at RT on a rotator with tubes upright. Primary antibody incubation was carried out in 1% PBT (typically 100  $\mu$ L per tube) for 4 h at RT, followed by two consecutive overnights at 4°C with continuous rotation. After primary incubation, tissues were washed four times in 1.75 mL of 1% PBT for 15 min each.

Secondary antibody incubation was performed in 1% PBT (100  $\mu$ L per tube) for 4 h at RT, followed by 1–2 overnights at 4°C with continuous rotation. Post-secondary washes were performed four times in 1.75 mL of 1% PBT for 15 min each. An additional blocking step with 5% Normal Mouse Serum (NMS; Jackson ImmunoResearch, #015-000-120) in PBT was carried out for 1.5 h at RT prior to overnight incubation with at 4°C with the conjugated antibody. Following incubation, samples were washed four times in 1.75 mL of 1% PBT for 15 min each.

For mounting, tissues were placed on poly-L-lysine (PLL)-coated coverslips. Samples were dehydrated through a graded ethanol series (30%, 50%, 75%, 95%, and three changes of 100%), soaking for 10 min at each step. Tissues were cleared by immersion in three sequential 5 min xylene baths. Finally, samples were embedded by applying 4–5 (80  $\mu$ l)

drops of dibutyl phthalate in xylene (DPX) to the mounted tissue, placing the coverslip (DPX side down) onto a prepared slide with spacers, and applying gentle pressure to seat the coverslip. Slides were left to dry in the hood for 1–2 days prior to imaging.

### 2.3.4 Imaging

For imaging, the Zeiss LSM 780 was used.

### 2.3.5 Matching LM images with Seymour Data

## 2.4 Loss-of-Function Behavioural Assays

### 2.4.1 Fly strains

The following effector lines were used: UAS-impTNT-HA, UAS-TNT-HA, obtained from the Bloomington Stock Center (Indiana, USA).

We used the following split-GAL4 GMR driver lines: SS01978, SS26146, SS2856, SS22965, SS04497, SS25740, SS27197, SS36847, SS55970 (HHMI Janelia Research Campus; (Li et al., 2014; Meissner et al., 2025)).

### 2.4.2 Behavioural Experiments

9 split GAL4 lines were used and crossed with either UAS-TNT (effector) or UAS-impTNT (control) genetic driver lines lines. The cross was set at 25°C and the flies were laid on fly food for 3 days. Larvae containing the UAS-TNT or UAS-impTNT transgene were raised at 18°C for 7 days with normal cornmeal food. Third instar larvae were used for all experiments.

Larvae were separated from food by using 15% sucrose and washed with water, then dried and placed in the center of the arena, consisting in 3% Bacto agar gel in a 25 × 25 cm square plastic plate. Experiments were conducted at 25°C. Larvae were monitored with the Multi-Worm Tracker (MWT) software (<http://sourceforge.net/projects/mwt>); (Ohyama et al., 2013).

For light-stimulation experiments, we used approximately 30 larvae for each run. The larvae were presented with green light for 40 seconds, and the amount of larvae turning was monitored before, during and after stimulus presentation. 6 runs were performed for every line.

### 2.4.3 Behavioural Quantification

Larvae were tracked in real-time using the MWT software. We rejected objects that were tracked for less than 5 seconds or moved less than one body length of the larva. For each larva MWT returns a contour, spine and centre of mass as a function of time. Raw videos are never stored. From the MWT tracking data we computed the key parameters of larval motion, using specific choreography (part of the MWT software package) variables<sup>28</sup>. From the tracking data, we detected and quantified crawling and rolling events and the speed of peristaltic crawling strides.

### 2.4.4 Behavioural Data Analysis

## 2.5 $\text{Ca}^{2+}$ Imaging with Light Sheet Microscopy

### 2.5.1 Fly lines

### 2.5.2 Sample Preparation

Fly larvae were raised on standard cornmeal-based food. Second instar larvae were selected for live imaging. Individual larvae were dissected in physiological saline. After being pinned dorsal side up in Sylgard-lined Petri dishes, a dorsal incision was made along the larval body with fine scissors. The body wall was pinned flat and internal organs were removed. The isolated Drosophila CNS was then dissected away, preserving the Rh5 photoreceptors which expressed fluorescence. Only CNS samples that expressed irfp were selected. The samples were then embedded in 1% low-melting temperature agarose in physiological saline at 36 °C. The agarose containing the CNS was drawn into a glass capillary with 1.4 mm inner diameter and 2.0 mm outer diameter, where the agarose quickly cooled to room temperature, forming a soft gel. The agarose cylinder was extruded from the capillary so that the CNS was optically accessible outside of the glass.

### 2.5.3 LSM and Functional Imaging

The SiMView software was used to locate the brain. There are 2 views, one from the back and from the front. The view was set to an angle that is as flat and central as possible. Imaging is with green (561nm) exciting jRGECO(present in the cytosol) which is the Ca reporter expressed pan neuronally, and with red is the IRFP(expressd in the nuclei) brightens the cell nuclei very well which allows you to see the cell position.

**2.5.4 Data Analysis****2.6 nomenclature**

# Chapter 3

## Results

*Parts of this section incorporate text from published work [The central complex of the larval fruit fly brain] (Lungu et al., 2025)*

### 3.1 Strategy for identifying CX neuropils in the larval brain

In searching for a putative larval central complex, I used an iterative strategy guided by circuit features, lineage origin, relative location and morphology of the adult central complex. Since the adult brain presents fused hemispheres at the midline whereas the larval brain is characterised by a midline commissure, I placed more emphasis on searching for circuit motifs rather than anatomical similarity, while preserving the relative spatial location of a CX neuropil as a constraint. I focused on the following key circuit features:

1. Integration of sensory inputs: I searched for synaptic pathways corresponding to the adult's for integrating visual inputs into the PB, EB, FB and NO (Hulse et al., 2021); and gustatory inputs into the FB.
2. Association between centers for memory and spatial navigation: I looked for the characteristic link between the MB, the center for associative memory, and CX neuropils, which includes synapses from MBONs (MB output neurons) to the FB, EB and NO in the adult fly.
3. Recurrent intra-CX connectivity, such as with columnar neurons relating the PB with the FB and EB, or with the NO.

### 3.1.1 Identifying larva CX neuronal lineages

The *Drosophila melanogaster* central brain consists of stereotyped neural lineages, developmental-structural units of macrocircuitry formed by the sibling neurons of single progenitor cells, the neuroblasts (Spindler & Hartenstein, 2010); a subset of these structures the CX (Pereanu et al., 2011). Starting with the currently identified set of quiescent, embryonic-born neurons present in the larval brain that develop into the adult CX during metamorphosis (Andrade et al., 2019) I identified larval brain neurons satisfying imposed connectivity rules as per known circuit patterns across the adult CX neuropils (Franconville et al., 2018; Hulse et al., 2021; Wolff & Rubin, 2018; Wolff et al., 2015) (see 1.4) .

The hemilineages DM1, DM2, DM3, DM4, DM5 and DM6 are the core contributing lineages to the adult central complex columnar neurons (Table 1.2), and were therefore the first priority when searching for a putative CX at an earlier stage. I found that these lineages are present at the larval stage of drosophila under Ito Lee's naming in Table 1.2). Several neuropil specific lineages (e.g. EBa1(DALv2) for the EB see 1.2) also exist at the in the larva. In total, 12 of the 15 lineages contributing to the adult CX also exist in the larva, under different naming., I found that 9 of them contribute neurons to the larval central complex, and they are summarised in (Table 3.1). I used these 9 lineages as a starting point to find a putative CX neuropils in the larva.

I broadened the search beyond these lineages based on the expectation that some larval neurons may have been recruited to CX structures but would later take another identity in the adult, as is known for larval MB neurons (Truman et al., 2023), on the basis of matching synaptic connectivity patterns as observed in the adult (see Section 1.4) ; for example, for EB Ring neurons I looked for neurons with recurrent axo-axonic synapses with each other and with Wedge neurons, where their axon is located at the most anterior end of the brain neuropil, at an intermediate dorso-ventral position just anterior to the MB medial lobe.

I found several neurons that satisfied said criteria, and were therefore classified as central complex neurons (see Section 3.2). A comprehensive list of their lineages as well as the above lineages is shown in Table 3.2.

Adult lineage	Larval lineage
DM1	DPMm1
DM2	DPMpm1
DM3	DPMpm2
DM4	CM4
DM5/DM6	CM1/3
DL1	CP23
EBa1	DALv2
LALv1	BAMv1
CREa1	BAmd1
CREa2	DALCm12
SMPad2	DAMd2/3
SIPp1	DPMpl12

**Table 3.1 Lineages of the Adult CX that also contribute neurons to the Larval CX** A selection of adult CX lineages that were found to contribute to the larval CX neuropils. Adult CX lineages names are listed in the first column, and their corresponding larval lineage nomenclature in the second column(Eckstein et al., 2024).

Larval lineages	PB.b	PB.d	FB.b	FB.d	EB.b	EB.d	NO.b	NO.d	Total
BAla12				2	2				4
BAla34			4					9	13
BAlp_ant		2			2			1	5
bamd1						1		2	3
bamd2_d			1						1
bamd2_v			3					4	7
bamv12_dor	1			1			2	5	9
BAmv12_dor	1			1			2	5	9
Bamv12_ven	1			1	2	2		1	7
BLAd-OL	2								2
BLA1				2					2
BLAV12_ant				2					2
BLP12						2			2
BLVp2		2							2
CM13_lat	2				4	2			8
CM13_med					2	2			4
CM4-vm				2				4	6
CPa			1						1
CPb					8	4			12
CPe				2				4	6
Dalcl12					16	22			38
Dalcm12-m						4		2	6
DALcm12-v		2		2			4	1	9
dall1	2		4						6
Dalv1	8			6					14
Dalv23					14			4	18
dplal1-3			2		3				5
dplc_post_med		4		2			4		10
DPLc5		6	1	2			3		12
DPMI_ant	3	2						3	8
DPMI12		3		2			2		7
DPMI34_post				1			1		2
DPMm1	4		14	2			4		24
DPMm2		3		2		2			7
DPMpl12		5	2	2					9
dpmpl3								1	1
DPMpm1			4	2		4			10
DPMpm2						2	2		4
Total	20	33	36	36	53	47	24	46	295

None of these lineages are exclusive contributors to the larval CX - i.e all of these lineages contribute neurons to other parts of the brain - however, there are a few (about 10) that contribute more than a fifth (20%) of their neurons to CX neuropils, and are summarised in Figure 3.3.

Lineage	Left Hemisphere	Right Hemisphere	CX neurons	CX % of Lineage
Dalcl12	25	27	38	73.08%
DALv1	11	11	14	63.64%
dplc_post_med	6	10	10	62.50%
DPMl12	13	2	7	46.67%
Dalv23	18	21	18	46.15%
DPLc5	13	14	12	44.44%
dplal1-3	2	12	5	35.71%
CPb	14	20	12	35.29%
DPMm1	38	47	24	28.24%
dall1	9	18	6	22.22%

Table 3.3 **Lineage contribution to CX** Lineages contributing more than 20% of their neurons to the CX are captured, alongside their distribution across the left and the right hemispheres. The percentage represents the ratio between the total number of cells in an individual lineage divided by the number of neurons contributing to CX neuropils (axons, dendrites or both).

### 3.1.2 Connectivity of CX neurons

When investigating circuit motifs across the larval CX, I explored connectivity with established brain regions, starting with sensory input areas such as the Optic lobe(OL), and progressing to regions such as the MB, the LAL and the Lateral Horn (LH). I categorised individual cells on the basis of the location of their processes: where a neuron receives synaptic input (location of its dendrites) and sends output synapses (location of its axons; for nomenclature see methods section 2.6).

#### Sensory Inputs

The central complex is known primarily for visual input processing, therefore in the larva I looked at neurons downstream of photoreceptors. I investigated cells immediately connected to visual projection neurons (vPNs) which are directly connected to photoreceptors. Several of these neurons have been catalogued as Protocerebral Bridge (see section 3.2.1) or Noduli(see section 3.2.4) neurons. In addition to visual input, I found that olfactory input is integrated by all the larval CX neuropils indirectly via the Lateral Horn(LH) and the Mushroom Body through convergence neurons(CNs; which integrate learnt valences from the

MB and innate valences from the LH (Eschbach et al., 2021)) or MB output neurons and MB input neurons 3.3. This is in line with previous findings about the CX being integrative across multiple sensory modalities (Hulse et al., 2021). Since Gepner et al., 2015 demonstrated that Larvae have to integrate visual and olfactory gradients, with convergence of these sensory systems before decision to act on them. I expected there would be a structure receiving input from these modalities and used information such as lineage membership to figure out if these could be central complex neurons.

### Connectivity between CX Neuropils and Accessory Structures

Columnar and horizontal neurons have stereotyped connectivity patterns within the CX, being connected between themselves or with other accessory structures (e.g.LAL). To be able to define these, I categorised them similarly to how they have been categorised in the literature. For naming, I adapted Wolff et al., 2015 nomenclature, and named them on the basis of the location of input synapses (.d for dendrites) and the location of their output synapses (.b for axonal boutons). Once the synapses for each neuron were mapped, I categorised them on the basis of their location within the CX neuropils and relative to accessory structures as per Figure 3.1. As such I divided them into Intrinsic Neurons(those whose inputs and outputs are located within CX neuropils), Local Neurons (cells whose inputs and outputs located within the same neuropil), Input Neurons (those that send only dendrites processes within the CX and output outside of it) and Output Neurons: Cells that send dendritic inputs outside of the CX but output onto the CX neuropils. Since the CX of the larva is numerically reduced, I grouped Intrinsic and Local neurons, and named these **Core CX neurons** for a more concise, cohesive analysis of the CX network. There are 15 pairs of CX core neurons, all of which are presented in Table 3.5. For a comprehensive understanding of the connectivity patterns of these neurons, they have been written in a nomenclature adapted from Wolff et al., 2015 (Wolff et al., 2015). I classified neurons using the suffixes ".b" (axon boutons) and ".d" (dendrites) for CX neuropils. Hence, a neuron annotated as NO.b projects its axon into the NO, and likewise, a neuron annotated as FB.d places its dendrites in the FB. As such, neurons that are both .b and .d for CX neuropils are the CX Core neurons.

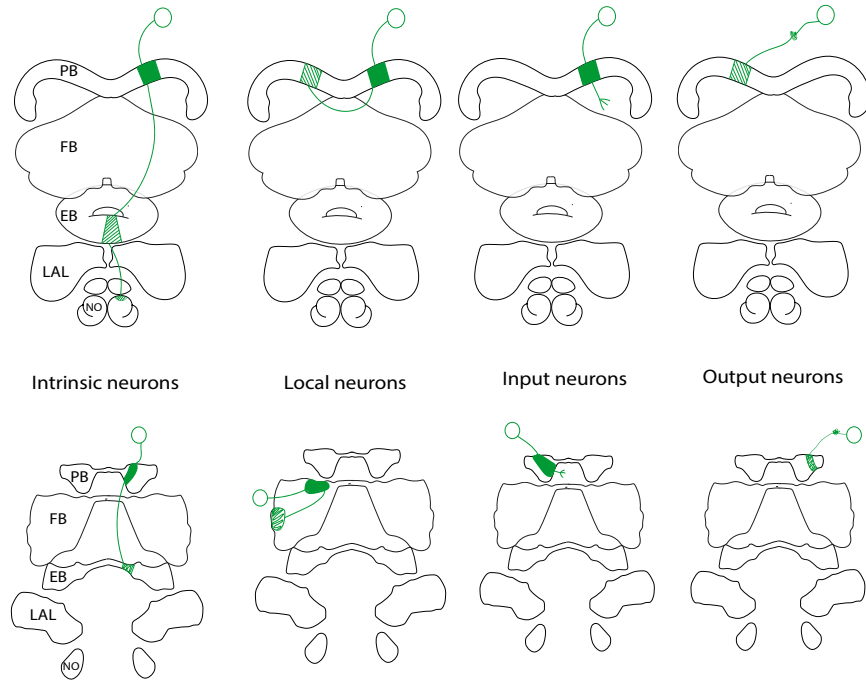


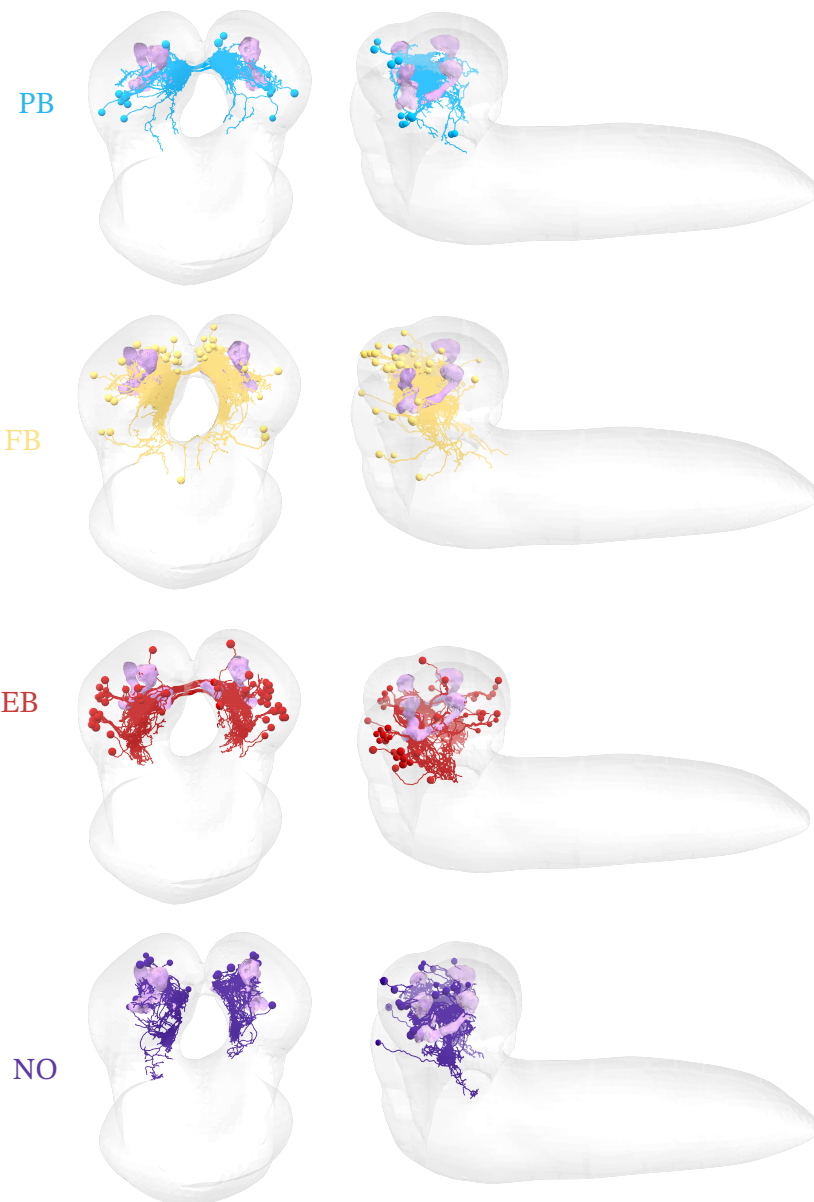
**Fig. 3.1 Classes of CX neurons** This schematic illustrates neuron classes of the adult CX (upper panel) and the larval CX (lower panel). The PB, FB, EB, NO and LAL are shown in each case to illustrate where a neuron arborizes. Neurons are drawn as a sketch, where the soma is represented by a green circle, the arbours are split into dendritic inputs - filled green boxed - and spiny axonal outputs - hashed scribbled green boxes. Cells are classified as either **Intrinsic Neurons**:neurons whose inputs and outputs are located within CX neuropils; **Local Neurons**: cells whose inputs and outputs located within one neuropil; **Input Neurons**: Neurons that have dendrites (receive synaptic input) located within the CX but output outside of it; and **Output Neurons**: Cells that receive inputs outside of the CX but output onto CX neuropils

Neuropil	PB	FB	EB	NO	LAL
PB	*	*	*	*	
FB	*		*	*	
EB				*	
NO		*		*	
LAL			*		
MBONs	*	*			

Table 3.4 **Monosynaptic connectivity between CX neuropils.** Asterisks indicate direct synaptic connections, with row neuropils synapsing onto column neuropils. The table summarizes the non-empty intersection sets for annotations in CATMAID such as FB.d with NO.b (i.e., neurons with dendrites in the fan-shaped body and axons in the noduli).

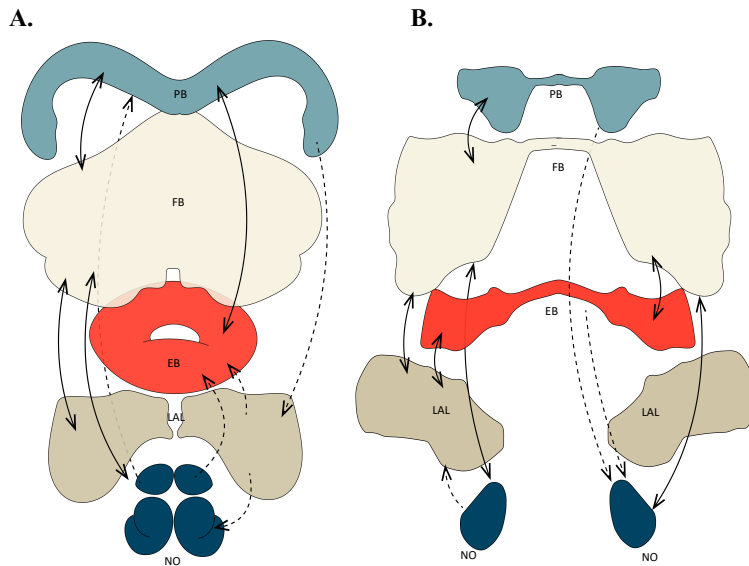
CX Core Neurons	Other Names (CX or MB)
FB.d, NO.b	FB-NO 1, FB.d.1
FB.d, PB.d, NO.b	FB.d.1, CN-34, MB2ON-119
FB.d, PB.d, NO.b	FB.d.1, MB2ON-204
FB.d, NO.b	FB.d.1, MB2ON-201
EB.d, EB.b, LAL.b	MB2IN-124, MB2ON-79
EB.d, LAL.d, EB.b	RN4, FBN-19, MB2IN-37, MB2ON-112
EB.d, LAL.d, EB.b	RN4, FBN-21, MB2IN-42, MB2ON-128
EB.d, EB.b	RN3, MB2IN-122, MB2ON-71
EB.d, EB.b	RN1/2a, FBN-20, MB2IN-38, MB2ON-115
EB.d, EB.b	RN1/2b, FB2IN-10, MB2IN-68, MB2ON-266
FB.d, FB.b	eDAN-2
FB.d, FB.b	MB2ON-125
FB.d, LAL.b	FB.d.2
PB.d, FB.d	FB.d.2
PB.d, NO.b	MB2ON-241

Table 3.5 **CX Core Neurons** The table illustrates, in the first column, the CX Core neurons in nomenclature adapted from Wolff et al., 2015(Wolff & Rubin, 2018), depicting the location of the dendrites (.d) axonal boutons (.b) in the Central Complex Neuropils. Each neuron is listed alongside their CX neuropil-specific nomenclature, and/or their MB nomenclature



**Fig. 3.2 Larval CX neuron boutons define the volumes of the 4 main CX neuropils.** Posterior and lateral views of neurons that contribute boutons ("."b") to each of the 4 neuropils. In concordance with the adult, the PB is the most dorsal and posterior neuropil of the whole brain; the FB occupies an intermediate medial position; the EB is the most medial anterior neuropil (same dorso-ventral level as the mushroom body medial lobe but even more anterior); and the NO are medial and ventral. Note that the white medial space in the larval cartoon is truly devoid of brain tissue: the larval CX neuropils line the medial boundary of the brain hemispheres, with the pharynx occupying most of the intermediate space.

### 3.2 The Central Complex of *Drosophila* Larva



**Fig. 3.3 The Central Complex Neuropils in Adult and Larva.** Dotted-line arrows represent unidirectional connections, filled-line arrows indicate bidirectional connections. In panel A. I show the adult *Drosophila* CX. Bidirectional connectivity is seen between PB-FB, PB-EB, FB-LAL and FB-NO, with unidirectional connections from NO-PB, PB-LAL, LAL-NO and NO-EB; Panel B. displays the larval *Drosophila* CX. Bidirectional connections are PB-FB, FB-EB, FB-LAL, FB-NO and EB-LAL; unidirectional connections are seen from NO-LAL, PB-NO and EB-NO. The volumes of the adult neuropils were adapted from (Franconville et al., 2018). The volumes of the larval neuropils were drawn via CATMAID using the .b and .d parts of the neurons contributing to each.

<b>PB</b>		<b><i>FB.d.2</i></b>	
<i>PB Horizontal</i>		ni contralateral 2	FB.d LAL.b
HF PB1_1	FB.d PB.b	ni contralateral 3	FB.d PB.d LAL.b
HF PB1_2	FB.d PB.b	ni contralateral 4	FB.d LAL.d
HF PB1_3	FB.d PB.b	<i>FB.d.3</i>	
HF PB2	FB.d PB.b	FB.d.3	FB.d LAL.b
<i>PB Columnar</i>		<i>FB.d.4</i>	
PB to NO	PB.d NO.b	FB.d.4	FB.b NO.d
PB to EB	PB.d EB.d LAL.b	<i>FB.d.5</i>	
<i>PB Intrinsic</i>		Pitch	FB.d PB.d NO.b
CN 35	PB.d.b	<i>FB.d.6</i>	
<b>EB</b>		Lure 3	FB.d PB.b
<i>EB Wedge</i>		<i>FB.d.7</i>	
W1-W8	EB.d.b	MB2IN 54/MB2ON	FB.d
<i>EB Ring</i>		<i>FB.d.8</i>	
RN1/2	EB.b	BLAI horseshoe	FB.d
RN3	EB.d.b	<i>FB.d.9</i>	
RN4	EB.d.b LAL.d	FB.d.9	FB.d PB.d LAL.b
<b>FB</b>		<i>FB Intrinsic</i>	
<i>FB Tangential</i>		e DAN2	FB.d.b
hs FB.1	FB.b	MB2ON 125	FB.d.b
hs FB.2	FB.b PB.b	<b>NO</b>	
hs FB.3	FB.b	<i>PB/FB to NO</i>	
hs FB.4	NO.d FB.b	FB NO	FB.d NO.b
hs FB.5	FB.b	CN 34	FB.d PB.d NO.b
hs FB.6	FB.b	MB2ON 204	FB.d PB.d NO.b
hs FB.7	FB.b	MB2ON 201	FB.d NO.b
<i>FB Columnar</i>		MB2ON 241	PB.d NO.b
<i>FB.d.1</i>		<i>NO Intrinsic</i>	
FB NO	FB.d NO.b	CN 6/16/61	NO.d.b
CN 34	FB.d PB.d NO.b	MB2ON 37	NO.d.b
MB2ON 204	FB.d PB.d NO.b	NO looper	NO.d.b
MB2ON 201	FB.d NO.b	<i>NO LAL</i>	
DPMpm1 bushy	FB.d	CN 37	NO.d LAL.b
		MB2INs/ONs	NO.d LAL.b

Table 3.6 **Central Complex Neurons of *Drosophila* Larva.** All the classes of neurons found in each neuropil of the larval CX are shown.

### 3.2.1 Protocerebral Bridge

In searching for the larval PB, I expected two sets of neurons: columnar and horizontal. In larva, four central complex lineages contribute columnar neurons, a subset of which position their dendrites at a posterior-dorsal location. I could not find a central complex lineage that would contribute horizontal fibres at a posterior-dorsal location necessary to intersect and synapse onto the dendrites of the PB columnar neurons; however, I found a larval lineage (DALv1) whose axons are bilateral and project to the appropriate area, and is developmentally related to another central complex lineage (DALv23). This suggests that neurons from non-central complex lineages may be recruited temporarily during the larval period, in a pattern reported so far for the mushroom body (see Discussion; (Truman et al., 2023)).

#### Larval PB Horizontal fibers

Among neurons of the DALv1 lineage, 4 left-right pairs (named HF-PB for "Horizontal Fibre PB") project their axons bilaterally and across the dendrites of the columnar neurons. 3 of the 4 pairs present an unusual axon configuration: first, they project contralaterally to drop their first output synapses, with the axon then crossing the midline a second time to return back to the same ipsilaterally corresponding location to again drop presynaptic sites . This peculiar axon configuration is unique among all neurons of the entire brain of the larva ((Winding et al., 2023)) and suggestive of potentially a delay line for comparing left-right sensory inputs. The 4th pair first drops presynaptic sites ipsilaterally and then its axon crosses the midline until reaching the corresponding contralateral location to synapse again (3.4). These neurons are PB.b neurons since they contribute axonal boutons to the PB. Several of these neurons have their dendrites enclosed in the FB (are FB.d neurons), making them Core CX neurons.

The presynaptic outputs of DALv1 neurons are symmetric, in that they contact the same homologous pairs of left-right neurons which are predominantly neurons of the columnar system from the DM1-DM4 lineages.

The axons of these 4 pairs of HF-PB neurons are tiled dorso-ventrally, falling into two bilaterally symmetric groups which I interpret as defining 2 + 2 bilaterally arranged PB compartments, each innervated by 2 pairs of axons (Figure 3.4C).

The dendrites of these 4 pairs of DALv1 neurons (HF-PB) are ipsilateral and dorsal, receiving polysynaptic inputs from vision and olfaction, like in the adult PB ((Hulse et al., 2021)). In the larva, I found that these multi-sensory inputs to the horizontal fibres of the PB are mediated by Convergence Neurons (CN-53 and CN-54, among others; (Eschbach et al., 2021)) that, as their name indicates, integrate inputs from both Mushroom Body

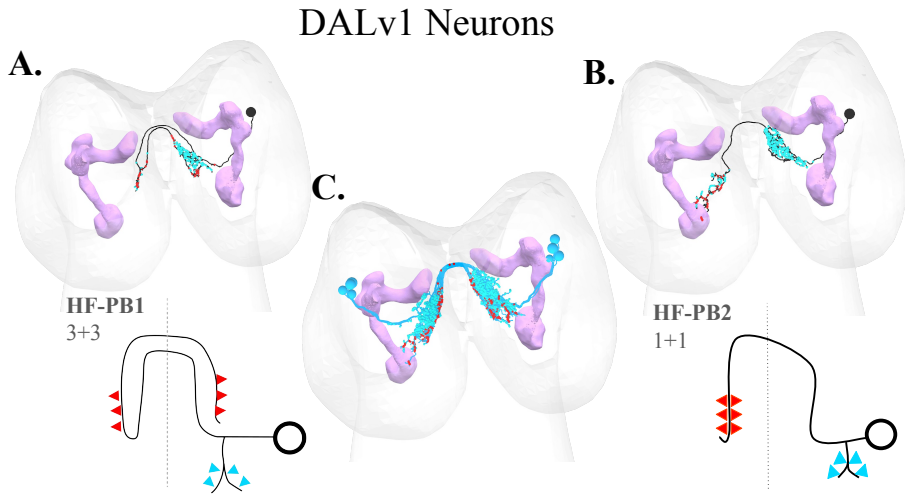


**Fig. 3.4 PB Horizontal Fibres (HF-PB).** Two types of horizontal fibre neurons are shown, each with a morphological reconstruction (top) and a simplified schematic (bottom). The mushroom body is shown in magenta. Input synapses (dendrites) are indicated by blue arrows, while output synapses (axons) are indicated by red arrows. Panel **A.** shows the 3 pairs of HF-PB1 neurons, characterized by a double-crossing axon; panel **B.** displays the single pair of HF-PB2 neurons, with outputs projecting only contralaterally; and panel **C.** the four bilateral pairs of HF-PB neurons shown together.

Output Neurons (MBONs) and from the Lateral Horn (LH) such as olfactory and visual PNs (Eschbach et al., 2020)). This circuit architecture indicates that sensory inputs arriving to the larval PB will have been modulated or gated by previously established associative memories, with implications for spatial navigation.

Three more larval lineages contribute HF-PB neurons: the BLAvm (neuron SLR), the BLAd-OL (neuron MB2ON-63), and the DPMm2 (neuron ADC1), with one pair of neurons each. MB2ON-63 presents a bilateral axon similar to the 4th pair of HF-PB (DALv1), and an ipsilateral dendrite that integrates inputs from multiple convergence neurons (CN-54, CN-9), MBONs (MBON-c1, MBON-d1), and sensory PNs (olfactory mPN B1, visual PVL09).

SLR presents a contralateral axon that spans both the FB and PB, and an ipsilateral dendrite that integrates inputs from MB2ON-63, CN-9, and the FB intrinsic neuron MB2ON-175 (see below), in addition to a long tail of weaker input from ascending neurons relaying information from the somatosensory system. This neuron was also proved to be dopaminergic (e-DAN6, see Section 3.6).

ADC1 presents an ipsilateral dendrite projecting to the posterior brain and a bilateral axon circumscribed to the PB. These neurons integrate inputs from multiple sensory PNs (mPN B2, mPN 5 (also known as mPN BAmd1-g), mPN A1, and weakly from others), a

convergence neuron (CN-35), MB2ON-94, and a few others weakly. Their axons target primarily HF-PB neurons (DALv1), but also convergence neurons (CN-56, CN-15, CN-35).

### Larval PB Columnar neurons

In the larva, the columnar system consists of neurons from 4 central complex lineages (DPMpm1, DPMpm2, DPMm1 and CM4) that also generate the columnar neurons of the adult (DM1, DM2, DM3 and DM4, correspondingly: these are the same lineages with different names for the larva and the adult for historical reasons). Larval columnar neurons present small, narrow dendrites circumscribed within the 2 + 2 compartments defined by the axons of the HF-PB (DALv1) neurons, from whom they receive synapses. These are catalogued as PB.d neurons since they contribute their dendrites to the PB.

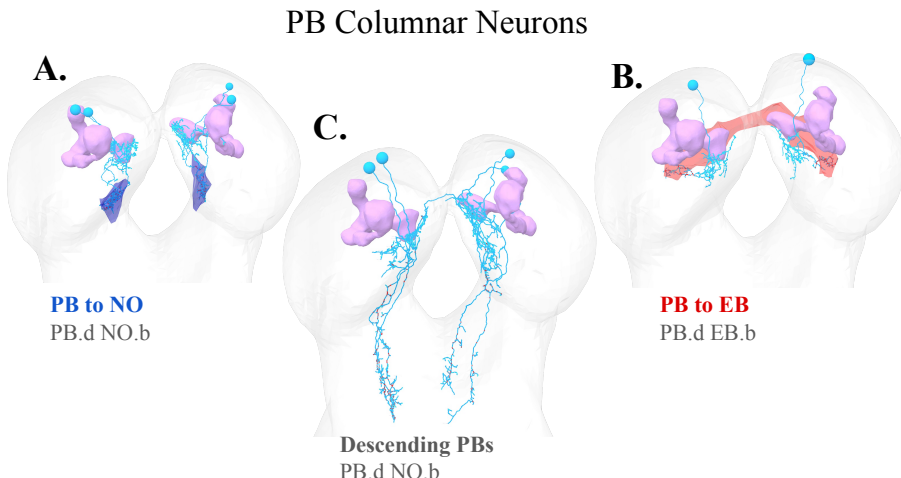


**Fig. 3.5 PB columnar neurons.** The three types of columnar neurons are shown. The mushroom body is shown in magenta. **A.** Neurons projecting from the PB to the NO (PB.d NO.b), with the NO neuropil shown in dark blue. **B.** Neurons projecting from the PB to the EB (PB.d EB.b), with the EB represented by the red structure beneath the mushroom body. **C.** Descending PB neurons projecting toward the SEZ or the VNC.

Among the columnar neurons, a subset project their axons directly to the NO (Fig. 3.5A), and another subset project directly to the larval EB (Fig. 3.5B).

I did not find among the larval columnar neurons any whose axon would project to more than one CX neuropil, despite such types being common in the adult (Hulse et al., 2021; Wolff & Rubin, 2018; Wolff et al., 2015).

Beyond the canonical columnar neurons projecting to other CX neuropils, I found some whose axons descend directly to the SEZ or nerve cord (Fig. 3.5C), and have been

accordingly named 'PB descending' neurons. (N.B. These neurons go on to connect to descending neurons, but aren't themselves descending neurons.

An additional group of CNs (CN-4, CN-23, CN-35, CN-54) send their dendrites to the PB. Notably, CN-35 sends both axons and dendrites to the PB, making it a **PB.d.b intrinsic neuron**. However these wouldn't be classified as columnar.

### PB Horizontal and PB Columnar connectivity

With the PB columnar neurons having dendrites enclosed in the PB (PB.d) and the PB horizontal neurons (HF-PB) sending output to the PB(PB.b), I expected there to be significant connectivity between the two types of neurons. Indeed a half of the HF-PB neurons are connected with columnar PB cells (3.7). Interestingly, only 2 pairs of neurons, both of HF-PB1 type, connected to every type of PB columnar neuron. Specifically a pair of HF-PB1 (annotated as HF-PB1\_1 in table 3.7) sends output synapses to 2 PB-NO (PB.d-NO.b) neurons, both of which are also second order MB output neurons (MB2ON-204 and MB2ON-241). The other pair of HF-PB1 (HF-PB1\_2) send outputs to 1 PBtoEB (PB.dNO.b) neuron, which is a second order MB input neuron (MB2IN-195), as well as 2 pairs of PB Descending neurons.

PB Horizontal	PB Columnar									
	PB to NO, MB2ON-204 _l	PB to NO, MB2ON-204 _r	PB to NO, MB2ON-241 _l	PB to NO, MB2ON-241 _r	PB to EB, MB2IN-195 _l	PB to EB, MB2IN-195 _r	PB Descending _1_l	PB Descending _1_r	PB Descending _2_l	PB Descending _2_r
HF-PB1_1_r					1	13	15	22	26	
HF-PB1_1_l					1	11	9	23	27	
HF-PB1_2_r	12	21	17		8	10	9	13	13	18
HF-PB1_2_l	17	22	7		8	11	14	10	13	19

**Table 3.7 PB horizontal fibres (HF-PB) connectivity to PB columnar neurons** A connectivity matrix representing connections from HF-PB neurons (rows) to PB columnar neurons (columns) is shown. Only the the two pairs of HF-PB1 (written here as HF-PB1\_1 and HF-PB1\_2) which send connections to PB columnar are presented. Neuron pairs are split in left (\_l) and right (\_r) cells for a more comprehensive understanding of the strength of connections. The left neuron from pair MB2ON-241 (5th column) has missing synapses because these haven't been traced yet, however these are considered present given reliability of the right one.

### 3.2.2 Ellipsoid Body

#### Larval EB Wedge neurons

In the larval brain, I found a group of 8 pairs of reciprocally synaptically connected neurons from larval lineage DALcl12, known to produce Wedge neurons in the adult, so I named them Wedge neurons (or W1-W8). Both their dendrites and axons are very small, and tiled medio-laterally, defining 8 compartments with one single neuron pair contributing to each (Fig. 3.6C). I found an additional pair of neurons from larval lineage DALv23 (which produces ring neurons in the adult) with the same connectivity pattern as Wedge neurons (Fig. 3.6B). All wedge neurons contribute both axons and dendrites to the EB, ,making them EB.d.b neurons, and Core CX neurons, accordingly.

While Wedge neurons make both axo-dendritic and axo-axonic synapses onto each other (like the AL Picky LNs do; (Berck et al., 2016); see Table3.7), their dendrites integrate inputs from a variety of sources, including MBONs (MBON-e1, MBON-e2, MBON-g1, MBON-g2, MBON-b3, MBON-m1, and weak inputs from more), convergence neurons (CN-14, CN-25, CN-62, CN-38), and MB feedback neurons (FBN-13, FBN-19, FBN-21), indicating that the EB is intimately and intricately involved with the MB (see below). Wedge neurons, like the adult, receive further axo-axonic synapses from Ring neurons (see below; RN1/2, also known as FBN-20; and RN3).

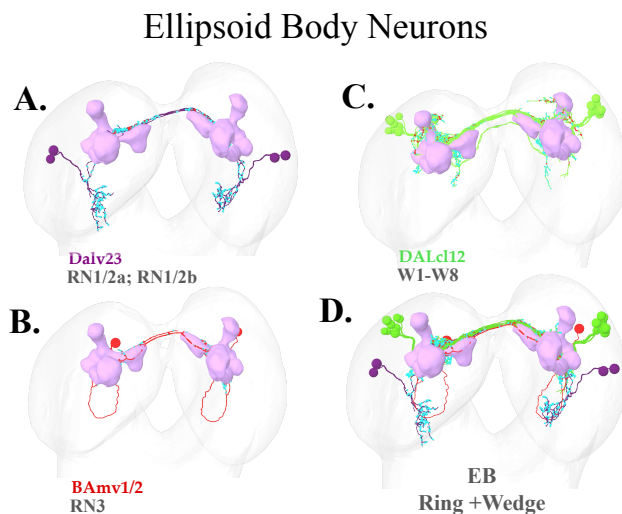


**Fig. 3.6 Ellipsoid Body Neurons.** Ring and Wedge Neurons with their corresponding lineages are shown. The mushroom body is coloured in magenta as a landmark in the larval brain. **A.** Ring neurons of lineage Dalv23, namely RN1/2a and RN1/2b; **B.** Ring neuron RN3 originating from lineage BAMv1/2; and **C.** The 8 EB wedge neurons (W1-8) originating from DALcl12 lineage. Panel **D.** depicts all these neurons stacked together to form the EB

**Larval EB Ring neurons**

I found one pair of neurons (RN3) of the larval BAmv1/2 lineage (corresponding to adult lineage LALv1 known to generate ring neurons) that receive visual input via PB columnar neurons, and reciprocally synapses axo-axonically with larval Wedge-neurons (Fig. 3.6A). Their axons are fully contained within the space defined by the wedge neurons. Similarly, I found two pairs of neurons (RN1/2) from the larval DALv23 lineage (adult EBa1 lineage, also known to generate ring neurons), synaptically connected like RN1/2 (Fig. 3.6B). I classified all of these as larval EB Ring neurons, all of them having both dendrites and axons inside the EB, making them EB.d.b neurons, and as such, CX Core neurons.

There were also 2 pairs of RN4 neurons, of lineage CM1/3, which have both dendrites and boutons in the EB, making them an EB.d.b intrinsic neuron, in addition to sending dendrites to the LAL.

Neuron	RN1/2a_l	RN1/2a_r	RN1/2b_l	RN1/2b_r	RN1/2b_r	RN3_l	RN3_r	W1_l	W1_r	W2_l	W2_r	W3_l	W3_r	W4_l	W4_r	W5_l	W5_r	W6_l	W6_r	W7_l	W7_r	W8_l	W8_r
RN1/2a_l	0	0	0	0	0	0	0	1	3	2	1	0	0	1	3	0	0	0	0	0	0	0	0
RN1/2a_r	0	0	0	0	0	0	0	0	1	3	0	0	0	0	0	0	0	0	0	0	0	0	0
RN1/2b_l	0	0	0	0	0	0	0	0	0	2	1	0	0	0	0	0	0	0	0	0	0	0	0
RN1/2b_r	0	0	0	0	0	0	0	0	0	0	3	0	0	0	0	0	1	0	2	0	0	0	1
RN3_l	0	0	0	0	0	0	0	0	2	0	0	0	1	0	1	0	1	0	0	0	1	0	1
RN3_r	0	0	0	0	0	0	0	0	2	1	0	0	0	0	0	0	0	0	0	0	0	0	0
W1_l	0	0	0	0	0	0	0	1	0	0	0	0	0	0	0	0	0	0	0	0	0	0	0
W1_r	0	0	0	0	0	0	0	0	1	0	0	0	0	1	0	0	0	0	0	0	0	3	0
W2_l	0	0	0	0	0	0	0	0	0	0	0	0	0	0	0	0	0	0	0	0	0	1	0
W2_r	0	0	0	0	0	0	0	0	0	0	2	0	1	0	1	0	0	0	0	0	0	0	3
W3_l	0	0	0	0	0	0	0	0	0	0	0	0	0	0	0	0	0	0	0	0	1	0	0
W3_r	0	0	0	0	0	0	0	0	0	0	0	1	0	0	0	0	0	0	0	0	0	0	0
W4_l	0	0	0	0	0	0	0	0	0	0	5	0	0	0	0	0	0	0	0	0	0	0	0
W4_r	0	0	0	0	0	0	0	1	0	1	0	0	0	0	0	0	0	0	0	0	0	0	0
W5_l	0	0	0	0	0	0	0	0	0	0	0	0	0	0	0	0	0	0	0	0	0	0	0
W5_r	0	0	0	0	0	0	0	0	0	0	0	0	0	0	0	0	0	0	0	0	0	0	0
W6_l	0	0	0	0	0	0	0	1	0	0	4	0	0	0	0	0	1	0	0	0	0	0	0
W6_r	0	0	0	0	0	0	0	0	0	0	5	0	0	0	1	0	0	0	1	0	0	0	0
W7_l	0	0	0	0	0	0	0	0	0	0	0	0	0	0	0	0	0	1	0	0	0	0	0
W7_r	0	0	0	0	0	0	0	0	0	2	0	1	0	0	0	0	0	1	0	1	0	1	0
W8_l	0	0	0	0	0	0	0	0	0	0	0	0	0	0	0	0	0	0	2	0	0	0	1
W8_r	0	0	0	0	0	0	0	0	0	0	0	0	0	0	0	2	0	0	0	2	0	0	0

Neuron	RN1/2a_l	RN1/2a_r	RN1/2b_l	RN1/2b_r	RN3_l	RN3_r	W1_l	W1_r	W2_l	W2_r	W3_l	W3_r	W4_l	W4_r	W5_l	W5_r	W6_l	W6_r	W7_l	W7_r	W8_l	W8_r	
RN1/2a_l	1	0	3	1	0	1	0	1	0	1	0	1	0	1	0	1	0	1	0	1	0	1	0
RN1/2a_r	2	0	2	3	0	0	0	0	1	0	1	0	1	0	0	0	0	0	1	0	1	0	0
RN1/2b_l	7	3	0	9	2	2	0	2	0	0	1	2	1	0	0	0	0	2	0	1	0	3	0
RN1/2b_r	3	3	9	0	0	0	0	0	0	0	0	0	0	0	1	0	0	1	1	1	0	1	0
RN3_l	0	0	3	0	0	4	0	0	0	0	0	2	0	0	0	0	0	1	2	0	0	1	0
RN3_r	2	1	0	0	9	0	0	0	2	0	0	0	0	0	0	0	0	0	0	1	0	0	0
W1_l	1	4	2	4	0	0	1	1	0	0	0	0	0	0	0	0	0	0	0	0	0	0	0
W1_r	2	0	7	7	0	2	0	0	0	0	0	0	0	0	0	0	1	0	0	0	0	0	0
W2_l	0	2	1	0	0	0	0	0	1	0	0	0	0	0	0	0	0	2	0	0	0	5	0
W2_r	6	1	1	4	2	0	0	1	0	0	1	0	1	1	0	0	7	0	0	0	0	4	0
W3_l	0	0	0	0	0	0	0	0	0	0	1	1	0	0	0	0	0	0	0	0	0	0	0
W3_r	0	3	1	2	2	0	1	0	1	3	1	0	1	0	0	1	0	3	0	1	0	1	0
W4_l	1	1	2	2	0	0	1	0	0	0	0	3	0	0	0	0	0	0	0	0	0	0	0
W4_r	4	1	5	3	0	0	0	3	0	0	0	0	0	0	0	0	1	0	0	0	0	0	0
W5_l	0	0	0	1	0	0	0	0	0	1	0	0	0	0	0	0	0	0	0	0	0	0	0
W5_r	0	0	0	0	0	0	0	0	0	0	1	0	0	0	0	0	0	0	0	0	0	0	0
W6_l	5	6	5	5	1	1	1	0	0	0	1	0	1	0	0	0	0	0	2	0	0	0	0
W6_r	10	10	4	10	0	0	0	1	0	2	0	1	0	1	0	0	0	0	0	1	0	0	0
W7_l	0	0	2	0	0	0	0	1	0	1	0	1	0	0	2	0	0	0	0	0	0	0	0
W7_r	1	1	1	2	1	0	0	0	0	1	3	0	0	0	0	0	0	2	0	0	0	2	0
W8_l	0	0	2	2	0	0	0	0	0	0	1	0	0	0	0	0	0	0	0	0	0	0	0
W8_r	0	0	1	2	0	0	0	0	3	0	0	0	0	0	0	0	2	0	0	1	0	0	0

**Fig. 3.7 EB Neurons Connectivity.** Both tables display the connectivity patterns among ring and wedge neurons in the ellipsoid body (EB). Each neuron is separated into left (\_l) and right (\_r) counterparts to represent lateralization. **Upper table:** axo-dendritic connections (color-coded in the green spectrum). **Lower table:** axo-axonic connections (color-coded in the yellow spectrum).

**Additional EB.d Neurons** There are seven more pairs of EB.d (neurons that contribute presynaptic sites to the EB) that didn't fall under ring or wedge neuron categories. Two of these are MB Dopaminergic neurons (DAN-d1 and DAN-g1), another 3 are LAL neurons(I

refer to these as EB to LAL neurons) - these can be LAL.d LAL.b or LAL.d.b - and the last 2 are MB second order output neurons (see Appendix for more)

### **EB Ring Neurons and EB Wedge Neurons connectivity**

In the adult, a key feature of nearly all ring neuron types(ER1-6)is their dense interconnectivity. Since ER neurons send output processes within the CX (Hulse et al., 2021), I deduced majority of them are axo-axonic. Interestingly, this is the exact pattern I observe in the larval ring neurons (RN1/2, RN3), with all these 3 neurons being reciprocally connected axo-axonically (Table 3.7).

The larval EB wedge neurons (W1–W8) form a densely recurrent network, reminiscent of adult wedge EPG neurons. Every wedge pair is connected reciprocally, with the predominant motif being axo-dendritic synapses; axo-axonic contacts are also present but weaker and fewer in number.

Importantly, all eight wedge neuron pairs (W1–W8)synapse directly onto every identified ring neuron (RN1/2a,b and RN3), creating an all-to-all Wedge to Ring connectivity motif that closely mirrors the characteristic pattern observed in the adult EB (see Fig. 3.7). However, these connections are exclusively axo-axonic.This dense, reciprocal coupling likely supports distributed representations and recurrent dynamics within the larval EB.

A summary of the connectivity motifs is given below; full pairwise counts and the axo-axonic versus axo-dendritic decomposition are shown in Fig. 3.7.

#### **3.2.3 Fan-Shaped Body**

In the larva, I found a number of putative FB horizontal/tangential cells originating in lineages known to contribute neurons to the adult FB. Characteristically, most present a bilateral axon closely wrapping around the midline, and an ipsilateral dendrite positioned within the superior dorsal protocerebrum (dorsal anterior neuropil) where they integrate numerous inputs from MBON axons, a pattern specific to the adult CX. Among the various neurons with dendrites within this very medial neuropil, I find neurons from lineages known to contribute to the adult FB and whose axons project to the putative larval NO, EB, PB and LAL.

#### **Larval FB Tangential cells**

I found a diverse and large collection of larval FB tangential cell types. All types contribute synapses rather specifically to the FB and are hence labelled as FB.b, a defining feature across them all. The somas originate in a number of larval lineages whose adult homologues are known to contribute neurons to the adult FB (see above), but also a few from the nerve

cord, projecting their ascending axons directly to the FB such as the pCC neurons (a cell type first reported in grasshopper (Goodman et al., 1984) and later in the *Drosophila* embryo (Jacobs & Goodman, 1989)). The axons of the pCC project to the ipsilateral FB. The set of ascending neurons isn't complete, for the ventral nerve cord (VNC) remains incompletely mapped.

Among all neurons projecting their axons to the FB, many are brain neurons that do so with a typical bilateral horseshoe ('hs') axon, and hence I named them hs-FB, with a numeric label for each subtype.

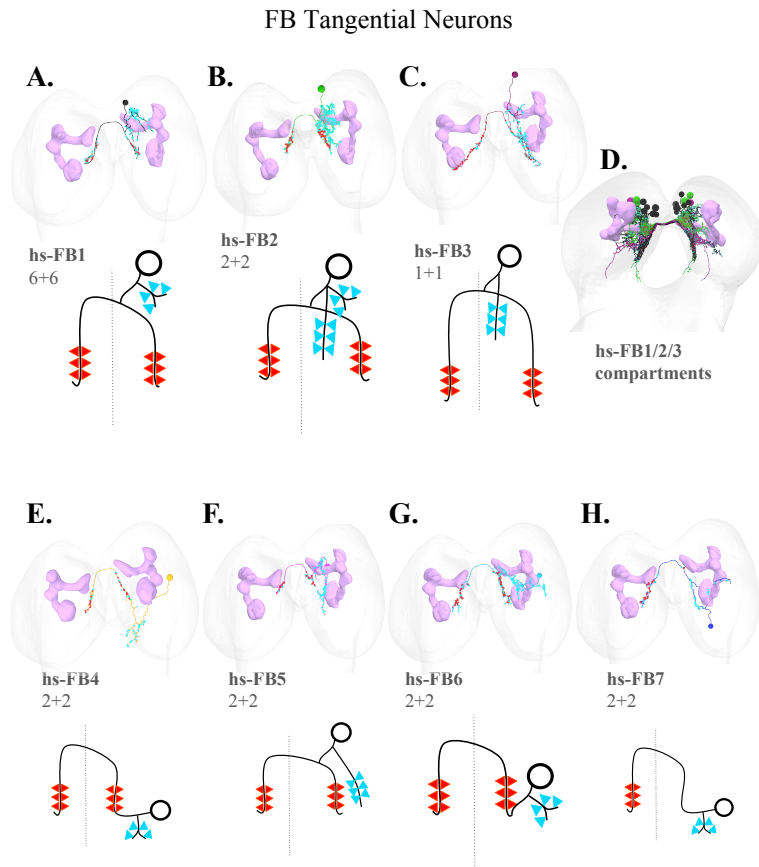


**Fig. 3.8 FB tangential cells**, also known informally as "horseshoe" neurons for the shape of their bilaterally axons. The seven hs-FB subtypes are shown, each with a morphological reconstruction (top) and a simplified schematic (bottom). Input synapses (dendrites) are indicated by blue arrows, and output synapses (axons) by red arrows. The mushroom body is shown in magenta. Neuron counts (left+right) are given below each schematic. **A–C.** Individual examples of hs-FB.1, hs-FB.2, and hs-FB.3. **D.** Overlay of hs-FB.1 through .3, illustrating the FB compartments they define. **E–H.** Individual examples of hs-FB.4 through .7.

The DM1-DM4 lineages that contribute to the adult CX also generate a number of FB tangential neurons in the larva (larval lineages DPMm1, DPMpm1, DPMpm2, and CM4-vm, respectively). Targeting the FB, there are several major subtypes.

First, 6 pairs of neurons (hs-FB.1) with a bilaterally symmetric axon that tightly lines the medial surface in a horseshoe shape, and with a smallish dendrite dorsal and slightly lateral to the FB, within the medial side of the superior protocerebrum (Fig 3.8A). Second, 2 pairs of neurons (hs-FB.2) also with bilaterally symmetric axons but that target the more

posterior-lateral FB and beyond into the larval PB, with also ipsilateral dendrites that extend anteriorly and ventrally along the neuraxis (Fig 3.8B). Third, a pair of neurons (hs-FB.3) with bilateral axons placed towards the most posterior end of the FB and perhaps beyond, into the lateral side, and with small ipsilateral dendrites (Fig 3.8C). The axons of all 6 pairs of hs-FB.1 neurons define the ventral layer of the FB, and the axons of the hs-FB.2 the dorsal one, which is shorter and more anterior. The hs-FB.3 axons project in between the other two types but also cover the posterior-dorsal area that hs-FB.2 doesn't (Fig. 3.8D). The larval BA<sub>La</sub>34 lineage generates sensory PNs, of which two pairs (hs-FB.4) present the typical bilateral axon and their dendrites collect inputs from the ventral posterior brain where ascending PNs from the somatosensory system (mostly mechanosensory) project their axons. One of the pairs is also NO.d (collects inputs from NO.b neurons) (Fig 3.8E). The larval BA<sub>Md</sub>2 lineage contributes two pairs of neurons (hs-FB.5) with a bilateral axon and dendrites that cover a region medial but lateral to the FB, and also far more ventral (Fig 3.8F). The larval DALI1 lineage contributes two pairs of neurons (hs-FB.6) with a bilateral axon and dendrites integrating inputs from the intermediate and lateral areas to the FB, primarily from neurons postsynaptic to ascending mechanoreceptive neurons like A00c (Ohyama et al., 2015). A number of neurons presynaptic to hs-FB.6 are also labelled as FFNs and MB2INs, meaning they converge onto MB DANs, MBINs and OANs (Eschbach et al., 2020) (Fig 3.8G). The larval CPa lineage contributes a pair of neurons (hs-FB.7) with a bilateral axon and dendrites that cover the most posterior end of the FB, or right outside, plus sparsely a space lateral to the FB, collecting inputs from polysynaptic pathways originating in somatosensory mechanoreceptive neurons (Fig 3.8H). Finally, the DPLal1-3 lineage contributes a pair of small neurons (ip-FB.1) with an ipsilateral-only axon targeting the most posterior lateral side of the larval FB, and with dendrites more lateral that integrate inputs from a variety of neurons, some of which are NO.d.

### Larval FB Columnar Neurons

By definition, all larval FB columnar neurons present dendrites in the FB (are FB.d), and are postsynaptic to FB.b neurons. I found a total of 9 types of FB.d neurons, all presented in Figure 3.9.

In addition to generating FB tangential neurons, the DM1-DM4 lineages also contribute 5 pairs of FB columnar neurons. These neurons (FB.d1) are characterized by ipsilateral-only dendrites largely circumscribed to the FB (except for the Bushy neuron from the DPMpm1/DM3 lineage), and projecting their ipsilateral-only clutched axons solely to the NO (so they are FB.d-NO.b). Therefore, FB.d.1 neurons are specialized in relaying information from the FB to the NO hemilaterally. Among FB.d.1, there are 3 MB related neurons, namely

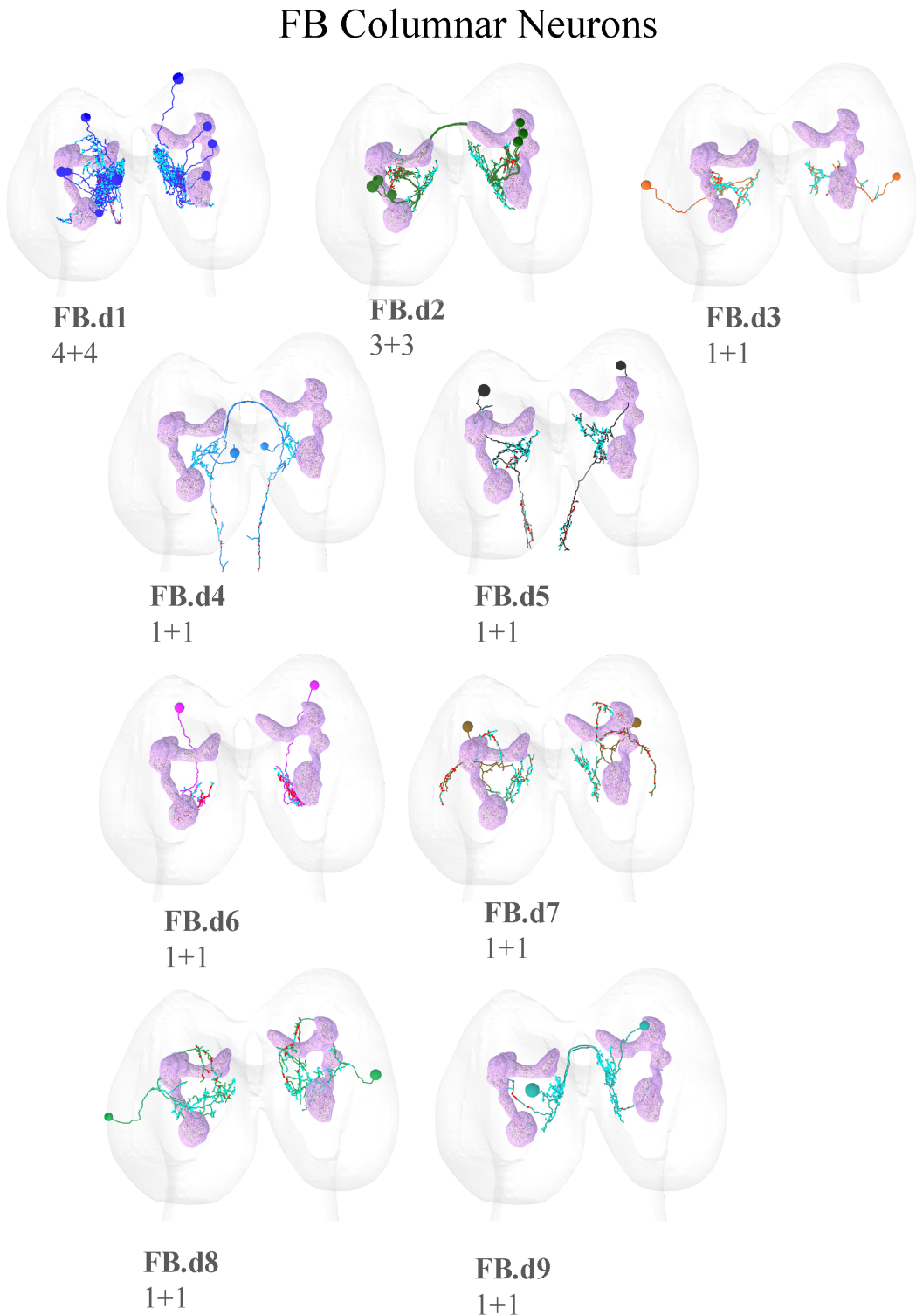


Fig. 3.9 **FB Columnar Neurons.** The 9 types of FB.d neurons are shown, and the number of pairs in case is displayed. The MB is coloured in magenta.

CN-34, MB2ON-201 and MB2ON-204 (Eschbach et al., 2021). One of the FB.d.1 was uncategorised so I named it FB-NO1, and the last one is known a descending neuron known as DPMpm1 bushy descending. Importantly, 2 of the 5 FB.d1 pairs also send their dendrites to the PB, making them PB.d neurons as well, therefore they are PB.d-FB.d-NO.b and also core cx neurons. This is the closest version to the adult PFN, however the adult analogue would be PB.d-FBb.b-NO.b.

The DM lineage (larval CM4-vm lineage) further contributes 1 pair of neurons (FB.d4) with ipsilateral dendrites in the posterior FB and beyond into an area adjacent to the LAL medially, and a contralateral axon that descends into the VNC, dropping presynaptic sites from the SEZ to the most posterior abdominal segments. Within the brain, FB.d.4 synapses onto some NO.d neurons (e.g., MB2ON-200) and also onto CN-28 (Eschbach et al., 2021)..

The MB neuroblasts contribute 3 pairs of early-born, non-Kenyon cell neurons (the 'ni' for "non-intrinsic"), named FB.d2, with ipsilateral dendrites in the FB and a contralateral axon targeting exclusively the LAL.

Then there are a collection of single pairs of neurons, each contributed by a different neuroblast, with dendrites in the FB and their axons targeting widely divergent neuropils, across the brain and also into the SEZ and VNC.

The larval BLAv12 lineage contributes 1 pair of neurons (FB.d3) with ipsilateral dendrites in the FB and also more medially, and ipsilateral axons targeting exclusively the LAL.

The larval DALcm12-v lineage (adult CREa1) contributes 1 pair of neurons (FB.d5) with ipsilateral dendrites in the FB and in the area adjacent but medial and ventral to the LAL, projecting their axons ipsilaterally from the NO to the medio-ventral brain and dorsal SEZ. The axons synapse onto a large number of NO.d neurons.

The BAmv12-dor larval lineage contributes 1 pair of neurons (FB.d6) with compact ipsilateral dendrites within the FB, and a compact short ipsilateral axon immediately dorsal on the PB. The FB.d6 hence serve as a direct relay from the FB to the PB, synapsing onto half a dozen PB.d neuron types.

The BALa12 larval lineage contributes 1 pair of neurons (FB.d7; also known as FFN-6, (Eschbach et al., 2021)) with compact ipsilateral dendrites in the FB, and an ipsilateral axon that targets the superior anterior protocerebrum where it synapses profusely onto the dendrites of DANs and OANs of the MB (DAN-i1, DAN-j1, DAN-c1, OAN-g1). Hence, FB.d7 serves as a relay between the FB and the MB input neurons, conveying teaching signals for associative memories.

The BLAl larval lineage contributes 1 pair of neurons (FB.d8) with ipsilateral dendrites within the FB but also extensively lateral to the FB, and with peculiarly curving axons that

follow the neuraxis, closely apposed to the dendrites of some hs-FB subtypes (hs-FB.1, hs-FB.2, hs-FB.3) and synapsing onto them.

The DPM12 larval lineage contributes 1 pair of neurons (FB.d.9, also known as FB-LAL1) with ipsilateral dendrites on the posterior hemilateral FB (with inputs from hs-FB.2, hs-FB.5, hs-FB.6) and also reaching into the PB (with inputs only from ADC1), and a contralateral axon targeting the LAL where they synapse onto LAL LNs, EB.d neurons, and multiple descending neurons (DNs) that project to the SEZ and VNC.

Finally, 3 of the 4 pairs of HF-PB neurons (the ones with a doubly crossing axon) are all FB.d, namely, they have dendrites within the FB and receive numerous synapses from FB.d neurons, in particular subtypes hs-FB.2, hs-FB.5 and hs-FB.6 (with further but weaker inputs from other subtypes). This indicates that the PB horizontal fibres not only integrate inputs from multiple sensory systems and gated by MB outputs, but are also modulated by the FB.

### Connectivity between FB Tangential and FB Columnar

In the adult, FB tangential neurons(FBt) arborize extensively across specific horizontal layers of the FB, conveying layer-specific synaptic inputs primarily sourced from accessory structures such as the CRE, SMP/SIP/SLP, and LAL, and have dense recurrence to the FB columnar FBc cells. Since in the larva there is a significantly numerically reduced FB, with no obvious layering and only one accessory structure structure (LAL), I couldn't draw straightforward analogies between the two networks, however I was curious if any general recurrence at all is present in the larval FB.

A significant recurrent connectivity across the larval FB is observed. All FB tangential neurons (hs-FBs) send synaptic outputs onto FB.d1, FB.d2 and FB.d7, and all except for one (hs-FB.3) synapse onto FB.b.8 neuron. There are 5 hs-FBs (1,2,5,6 and 7) synapse onto FB.d3 and 5 others (hs-FB.2,3,6,7,8) send processes to FB.d.9. Finally, FB.d.4, FB.d5 and FB.d6 receive input from 3 or less hs-FBs. A summary of this connectivity pattern is shown in Table 3.8.

### Larval FB intrinsic neurons

I found two pairs of neurons (MB2ON-125 and eDAN-2) that are both FB.d and FB.b, corresponding to the third type of adult FB neurons: the intrinsic.

MB2ON-125 integrate inputs across many neuron types, from PB.d columnar neurons to LH output neurons. As the MB2ON-125 name indicates (see (Eschbach et al., 2021)), it receives direct synapses from MBONs (just MBON-c1, but a strong connection). Fairly large, its dendrites span approximately the entire spatial domain of the putative larval FB.

		FB Columnar								
FB Tangential		FB.d.1	FB.d.2	FB.d.3	FB.d.4	FB.d.5	FB.d.6	FB.d.7	FB.d.8	FB.d.9
hs-FB.1		70	10	6	16	25		54	2	
hs-FB.2		145	68	24		43	8	2	19	30
hs-FB.3		35	19			19	18			1
hs-FB.4		3	4				21	1		
hs-FB.5		18	2	1				1	1	
hs-FB.6		166	41	11		6		1	19	18
hs-FB.7		63	16	10			8	50	1	19
hs-FB.8		8	4					5	1	1

Table 3.8 Connectivity between FB Tangential and FB Columnar neurons. Cell shading corresponds to relative connection strength (darker = stronger).

Postsynaptically I find the CSD neuron (Berck et al., 2016) and ascending neurons from the ventral nerve cord (VNC), among many others such as FFN-31 (so-called feedforward neurons, from the MB perspective, that bring sensory inputs to MB DANs; (Eschbach et al., 2021)).

The second FB.d.b, eDAN-2, is a non-MB dopaminergic neuron (DAN) entirely circumscribed to the posterior-lateral end of the FB. This neurons was identified via immunohistochemistry and is described at length in section section 3.6 on DANs of the CX below for details.

### 3.2.4 Noduli

In the larva I found a set of 21 neurons (10 pairs plus one unpaired) with highly compact, clutchy axons situated in the posterior ventral area of the brain, from lineages DPMm1 (DM1 in the adult), DALcm12, DPMl12, DPLc5, and BAMv12, as well as a few other larval lineages (Fig. 3.2). I define the volume encapsulating all their clutchy axons as the putative Noduli of the larval *Drosophila*, and labelled all these neurons as NO.b.

Among the 21 NO.b neurons in the larva I find several FB.d neurons (four pairs of the FB.d.1 subtype including CN-34) as well as a PB.d neuron (MB2ON-241) and convergence neurons (CN-6, CN-16/MBON-p1 (Eschbach et al., 2020) and CN-61), the latter of which also innervate the NO with their dendrites, making them intrinsic NO neurons (NO.d.b.). There were many neurons postsynaptic to MBONs (MB2ON-37, MB2ON-241), NO-looper (lineage BAMv12dor), MBON-p1 (a multi-compartment MBON of the MB vertical lobe; (Eichler et al., 2017)), and an unpaired neuron (DLPc lineage). Most NO.b neurons integrate inputs from the MB, as their names indicate (see (Eschbach et al., 2021)).

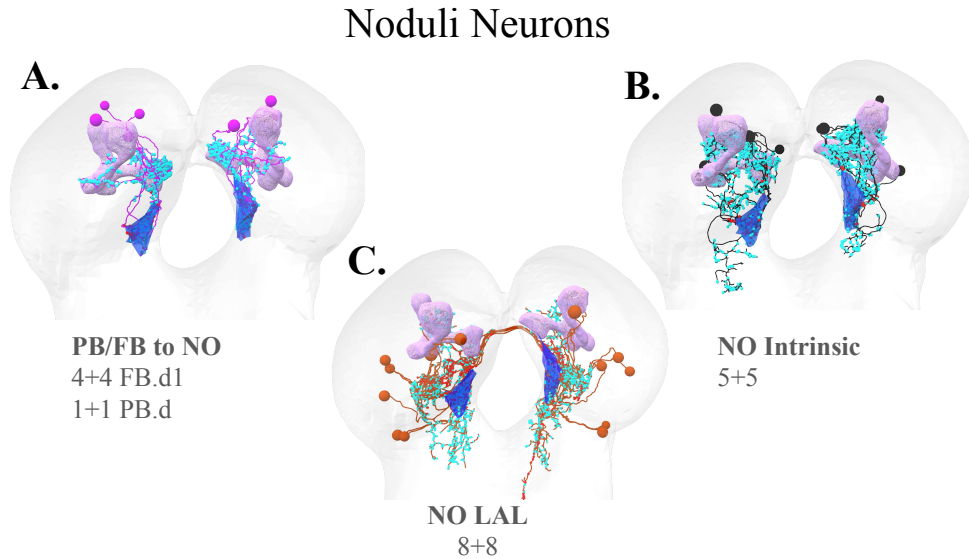


**Fig. 3.10 NO neurons.** The two types of NO.b neurons are shown. In panel A, the 4 pairs of FB.d1 neurons are displayed. In panel B, the MB related neurons (M2BONs and CNs) are presented. Panel C shows both of these combined. The MB is shown in magenta, and the volume circumscribing NO.b and therefore defining the Noduli is highlighted in dark blue under the MB

In addition to the 21 NO.b neurons described above, I identified approximately 92 neurons whose dendrites are located within the putative noduli (henceforth NO.d neurons). These NO.d neurons arise from a variety of larval lineages and can be grouped by their predominant connectivity and putative function. The major classes are: MB-related inputs and feedback neurons (many MB2INs/M2ONs/FBNs and convergence neurons(CNs) that convey learned-valence and feedback signals to the NO); LAL-projecting neurons that route processed NO signals to premotor or integrative centers; descending/SEZ-projecting neurons that relay NO-processed information toward motor circuits; and a small set of ascending or sensory-associated neurons that provide multisensory context.

Class	Approx. count
MB-related inputs (MBINs, FBNs, CNs)	38
Local interneurons / recurrent NO circuitry	20
LAL-projecting neurons	12
Descending / SEZ-projecting neurons	10
Ascending / sensory-associated inputs	7
Unclassified / other	5
Total (approx.)	92

Table 3.9 Approximate classification and counts of neurons with dendrites in the larval noduli (NO.d).

Functionally, the large fraction of MB-related NO.d neurons indicates that they are implicated in memory-modulated signals in the larva. The presence of many LAL- and descending-projecting NO.d neurons supports the idea that the noduli contribute to transforming MB-gated sensory or internal-state information into action-related commands. Not a single NO.d neuron projects its axon onto any of the other core larval central complex neuropil, but some project to the LAL (Table 3.4), supporting a role for the NO as an output neuropil of the central complex.

### 3.3 Mushroom Body and the larval CX

In the adult **Drosophila**, the Mushroom Body is known to output onto the Central Complex neuropils through the MB Output Neurons (MBONs). At this stage, adult MBONs primarily target the Fan-shaped Body - tangential neurons from the middle layers (4-6) - and the Noduli - via a direct glutamatergic connection from MBON-30 to LCNOp(LAL-NO) neurons which then target the PFN (PB-FB-NO) neurons (Hulse et al., 2021). Here, I examine the synaptic relationships between mushroom body input (DANs, MBINs, OANs) and output (MBONs) neurons and the larval central complex neuropils.

#### 3.3.1 A loop between FB and the 'c' compartment of the MB

I found that MBON-c1 synapses onto one FB.b neuron, MB2ON-125. Interestingly, DAN-c1 integrates inputs from an FB.d neuron, FFN-6, which in turn integrates inputs from a few neurons that are directly postsynaptic to MB2ON-125, defining a loop between the MB 'c' compartment and the FB. No other MBON supplies direct or two-hop inputs onto the FB.

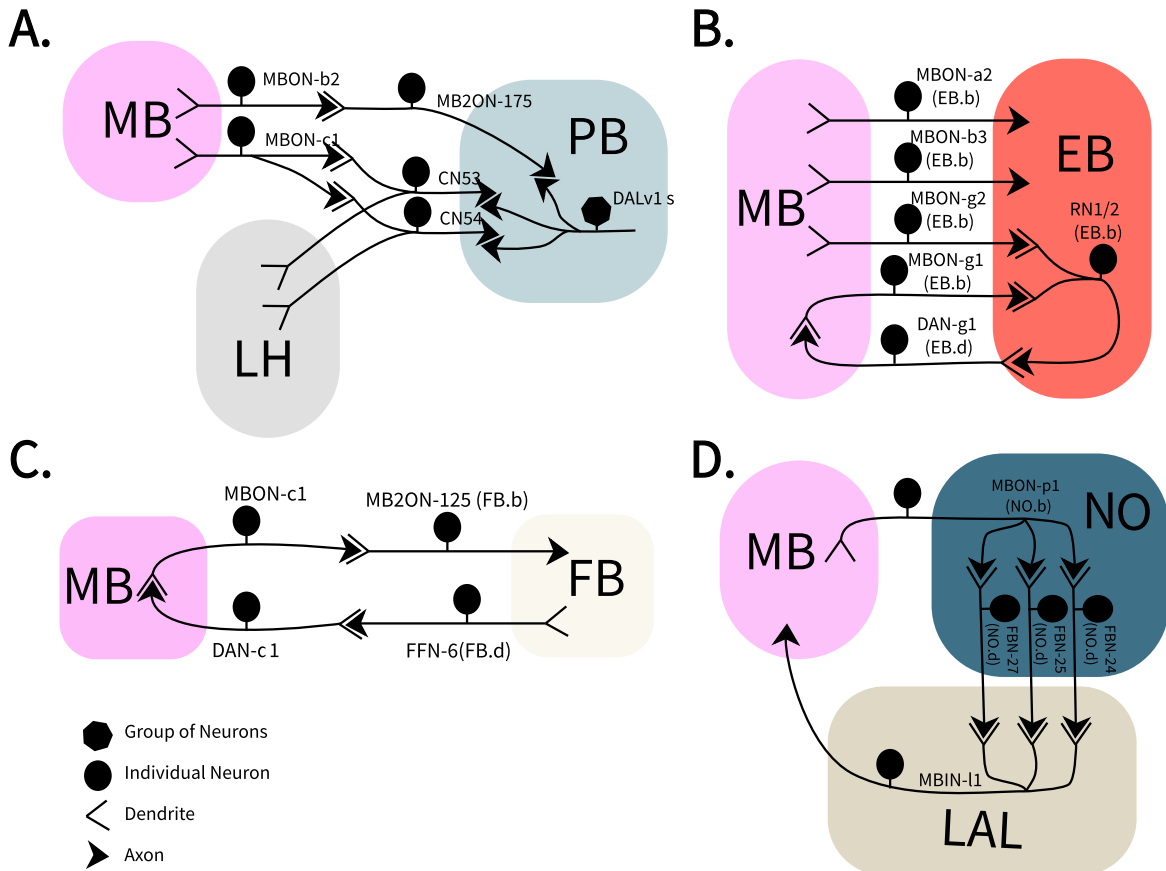


**Fig. 3.11 Mushroom Body Connections to the Larval CX.** Key connections between the larval MB and the larval CX neuropils are shown. Rounded shaped cartoons are used to illustrate different regions: light blue for PB and light grey for lateral horn (LH) (panel A.); red for the EB (panel B.); light beige for FB(panel C.); dark blue for NO (panel D.) and magenta for the MB.

### 3.3.2 Reciprocal connectivity between EB RNs and the 'g' compartment of the MB

Four MBONs (a2, b3, g1 and g2) are EB.b (i.e., deliver synapses to the EB; Fig. 3.11). Interestingly, some of these MBONs are monosynaptically interrelated, namely MBON-g1 and -g2 (which promote approach) are GABAergic neurons that synapse onto MBON-a2 (which promote avoidance) (Eschbach et al., 2021). Furthermore, MBON-g1 and -g2 synapse axo-axonically onto an EB ring neuron, RN1/2 (also known as FBN-20; (Eschbach et al., 2021)), a core GABAergic neuron of the EB, which in addition to synapsing axo-axonically reciprocally onto EB wedge neurons also synapses onto an EB.d neuron, DAN-g1. Therefore, the output of the MB 'g' compartment (MBON-g1 and -g2) modulate, with GABA, the axon of an EB ring neuron (RN1/2), which in turn synapses onto the dendrites of the teaching neuron of the MB 'g' compartment (DAN-g1). This circuit configuration defines a close relationship between an associative learning compartment (MB 'g') and the EB.

Assuming the larval ring neurons RN1/2 are also GABAergic, as they are in the adult (Hanesch et al., 1989), the MB 'g' compartment is providing disinhibitory input onto the EB, by means of MBON-g1/g2 inhibiting its ring neurons. This disinhibition could be understood as a learning-based gating mechanism over EB wedge neurons, with features of input space expressed in the Kenyon cell population code, by coincident activity with DAN-g1, modulating the activity of the EB wedge neurons that the ring neurons also synapse onto. Taken together, this implies that, if the larval EB is functionally similar to that of the adult EB, there is a component of learning built-in into the internal representation of the direction of movement.

### 3.3.3 A loop between the NO and the MB vertical lobe via LAL

MBON-p1 is a multi-compartment MBON of the MB vertical lobe that is an NO.b, (i.e., it delivers output synapses to the NO). At the NO, MBON-p1 synapses onto several NO.d neurons, FBN-24, FBN-25, and FBN-27, which are MB feedback neurons (Eschbach et al., 2020) that all project to the LAL and synapse strongly onto MBIN-11, a MB input neuron targeting multiple compartments of the vertical lobe. This circuit configuration defines a strong tight loop between the MB vertical lobe and the NO via the LAL. Note that the dendrites of MBIN-11 are entirely contained within the LAL compartment. In addition, these three feedback neurons also synapse weakly onto DAN-d1.

### 3.3.4 The MB modulates inputs to the PB

Multiple sensory modalities converge onto the horizontal fibres of the PB (DALv1 neurons) via MB convergence neurons (CN-53, CN-54) and a neuron postsynaptic to MBONs (MB2ON-175). These CNs were previously described as integrating the output of both the lateral horn (LH), which conveys innate pathways, and the mushroom body (MB), for associative memory (Eschbach et al., 2021). Synapses from CN-53, CN-54 and MB2ON-175 onto PB horizontal fibre neurons (DALv1) follow an intriguing pattern of synapsing onto either the dendrite or the axon, but largely not both, with specific target choices among the 4 DALv1 neurons. In considering that 3 of the 4 DALv1 neurons (PB horizontal fibres) present an unusual bilateral axon that first deploys output synapses contralaterally and then ipsilaterally (Fig. 3.4A), the observed pattern of selective axo-dendritic and axo-axonic connections has implications for the modulation of the output of the unusual axons of DALv1 neurons.

In summary, from the perspective of the PB, I find the following circuit architecture: the multi-sensory convergence onto the PB horizontal fibres is directly modulated by the MB, precisely because the neurons that mediate the multi-sensory convergence are themselves CNs (i.e., integrate also MBON synapses in addition to LH inputs): the CN-53 and CN-54. Both of these neurons are also Lateral Horn (LH) neurons. Notably, CN-54 is in addition a PB.d neuron, integrating inputs from PB horizontal fibres (DALv1 neurons).

Upstream of these convergence neurons, among various MBONs, MBON-c1 is the most strongly connected to both CN-53 and CN-54, which also integrate inputs from MBON-b1 and MBON-b2. All three are MBONs of the MB peduncle; MBON-c1 has no known function, while MBON-b1 and MBON-b2 promote approach (Eschbach et al., 2021).

Importantly, the axon of MBON-c1 receives direct presumably inhibitory (GABAergic) inputs from MBON-g1, MBON-g2, and MBON-d1, with all three MBONs participating of circuit loops with other central complex neuropils.

Additionally, neurons directly postsynaptic to MBONs, such as MB2ON-175, in turn directly synapse onto the horizontal fibres of the PB, either axo-axonically or axo-dendritically, in a pattern selective of specific DALv1 neurons.

Overall, I observe that not only are navigational decisions - such as whether to turn towards a stimuli or not - proceeding co-dependently per sensory modality but they are also integrated across modalities, an observation that is in line with previous behavioural experiments (Gepner et al., 2015). Importantly, this integration is modulated by prior memories. (vis the MB).

### 3.4 Visual Input into the larval CX

In the adult, the CX is primarily involved in visually guided behaviour and is a core hub for visual information processing (Hulse et al., 2021; Omoto et al., 2017); hence I was curious if there whether the same concentration of visual inputs - and in what architecture - exists in the larva larva. The larval *drosophila* doesn't actually have eyes, however it does have 2 photoreceptor(PR) classes: Rhodopsin5-PRs (Rh5-PRs) which detect blue light and are critical for rapid avoidance 1 (Keene et al., 2011); and Rhodopsin6-PRs (Rh6-PRs) which primarily detect green light. The larval visual circuit, terminating in the larval optic neuropil (LON), includes two types of downstream interneurons: Visual Projection Interneurons (VPNs) and Visual Local Interneurons (VLNs). Whilst PRs synapse onto both, Rh5-PRs preferentially synapse onto VPNs (90% of Rh5-PR targets are VPNs). whereas Rh6-PRs principally synapse onto VLNs (79%), and much less onto VPNs (15%, specifically the Pdf-LaNs).

I investigated visual inputs towards the central complex from both VPNs (Fig. 3.12) and VLNs(Fig. 3.13) by looking connections immediately downstream of them as well as 2 hops away.

#### 3.4.1 VPNs inputs to the CX

Several VPNs (neurons that receive RH5-PR input) contact the FB neurons: pOLP, PVL09 (aversive behaviour neurons), nc1 and nc2. While no VPNs directly connect to the FB, these neurons first synapse onto convergence neurons CN-34, CN-50, CN-59, and MB2ON-54 as well as two downstream VPN neurons (down\_PVL09 and down\_pOLP) before reaching 6 FB tangential horseshoe neuron types (hs-FB1, hs-FB2, hs-FB3, hs-FB4, hs-FB5 and hs-FB6) which project their axons to the FB; as well as one FB.d.b neurons (MB2ON-125; Fig. 3.12 A).

In the adult, the EB is known to receive visual inputs via a polysynaptic pathways (see Fig. 6 in (Hulse et al., 2021), and Fig. 4 in (Omoto et al., 2018)). In the larva, I find that the main visual PN for negative phototaxis, PVL09 (Humberg et al., 2018), synapses axodendritically onto MB2ON-187, which relays sensory inputs from visual and other sensory modalities axo-axonically onto all of larval Ring neurons. MB2ON-187 is named so for being postsynaptic to MBONs (MBON-c1 in particular; (Eschbach et al., 2021)). Through MB2ON-187, multiple sensory PNs (PVL09, mgPN 7) and many neurons postsynaptic to MBONs (MB2ONs) synapse onto Wedge neurons. (Fig. 3.12 B). The latter indicate, again, that MBONs modulate or filter sensory inputs converging onto the EB. The EB also receives input from pOLP - another VPN contributing to negative phototaxis - via a non-PB DALv1

neuron (DALv1 contralateral 4) which interestingly also receives input from PVL09. This interneuron targets an FFN8, a feedback neuron sending axons to the EB.

In the adult, processed visual information in the EB is transferred to PB columnar neurons. In the larva , I find that not only do PB Columnar neurons receive visual input, but also all the HF-PB DALv1 neurons do. Four PB columnar neurons receive visual input from PVL09, pOLP, nc1 and nc2 via CNs (CN-3, CN-26, CN-54, CN-57, CN-59) and MB related neurons (MB2IN-194 and MB2ON-175; Fig. 3.12 D1). All of HF-PB neurons (HF-PB1 and HF-PB2) receive input from VPNs, this time only from PVL09, nc1 and nc2. The information is sent via similar CNs (CN-26, CN-45, CN-53) as well as from MBON-175 (as for PB columnar and EB neurons above), and from MB2ON-63, which sends axons to the PB (Fig. 3.12 D2). Another, perhaps unexpected, visual hub in the larval CX is the NO. PVL09, as well as nc1 and nc2, which compute light intensity, synapse directly onto three NO.b neurons, two of which FB.d1 neurons, while the other is a neuron innervating dendrites in the PB. In addition, VPNs send indirect connections to three more NO.b neurons which are CNs (CN-6, CN-16, CN61) via two (again!) CNs(CN-45 and CN-53) and two MB2INs (MB2IN-144 and MB2IN-210). (Fig. 3.12 C).

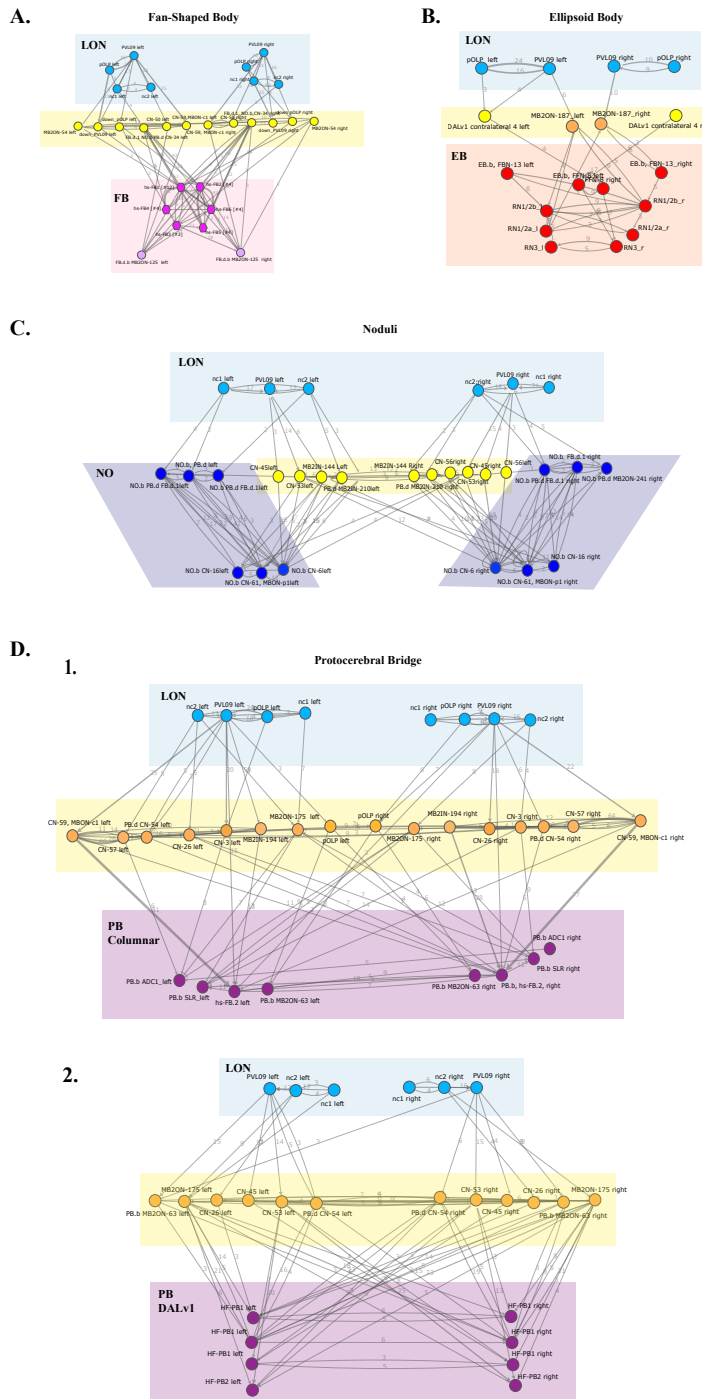


**Fig. 3.12 VPNs Input to the Larval Central Complex.** The inputs from visual projection neurons (VPNs) towards each larval CX neuropil are shown. In each case, neurons are coloured to represent anatomical regions: VPNs are highlighted in a blue rectangle to represent the larval optic neuropil (LON), whilst the layer of interneurons connecting VPNs to the CX are highlighted in yellow. Individual CX neuropils are coloured in magenta (FB), red (EB), dark blue (NO), and deep purple (PB). In each case, both .d and .b neurons are included in the analysis. Panel **A** displays VPN connections to FB neurons; panel **B** illustrates VPN inputs towards EB; panel **C** shows VPN circuits towards the NO; finally, panel **D** illustrates two separate figures for VPN input into PB columnar (**D1**) and PB horizontal fibres (**D2**) for ease of visualisation.

### 3.4.2 VLN inputs to the CX

Similar patterns of connectivity are found from VLNs (neurons mostly receiving input from RH6-PRs). Several PB neurons - HF-PB2 (which is also an FB.d neuron), MBONs (MBON-63, MBON-94, MBON-204 which is also an NO.b and FB.d1 neuron) and CNs (CN-35, CN-54) - collect input from one VLN, named 5thLN. A VPN(PVL09) is downstream of this VLN and facilitates transmission sensory input. Other interneurons include CN-15 and MB2ON-199 (Fig. 3.13 A).

The EB displays similar circuit patterns, with 5thLN being the only one sending sensory inputs to several EB.b neurons, interestingly, to none of the ring or wedge neurons, but to several MBONs (MBON-a2, MBON-b3, MBON-g1, MBON-g2) known to receive dopaminergic input from DANs with analogous names (Eschbach et al., 2020), as well as to two DANs themselves (DAN-d1 and DAN-g1). In addition CN-36 is also an EB.b that collects visual input (Fig. 3.13 B).

The larval FB collects visual input from 3 VLNs: LN1, LN4 and 5th LN. The information is sent via three MB-related neurons (MB2IN-209 MB2IN-162 MB2ON-175), one convergence neuron (CN150 and a lateral horn neuron LH-17, towards two FB tangential horseshoe neurons (hs-FB.1 hs-FB.2; (Fig. 3.13 C). and an FB.d1 neurons (MB2ON-204) which is also PB.d and NO.b.

Finally, the NO receives inputs from LN1, LN4 and 5th LN, mediated by KC LON, MB2ON-199 and CN-15 towards several neurons that send their clutched axons to the NO: MB2ON-204 (which is also a PB.d and a FB.d1), CN-61, CN-6 and CN-37 (which is also an LAL.b).

Interestingly, all neuropils seem to collect visual input from at least one VLN, reliably from the 5thLN, suggesting the larval CX must be implicated in processing of green light.

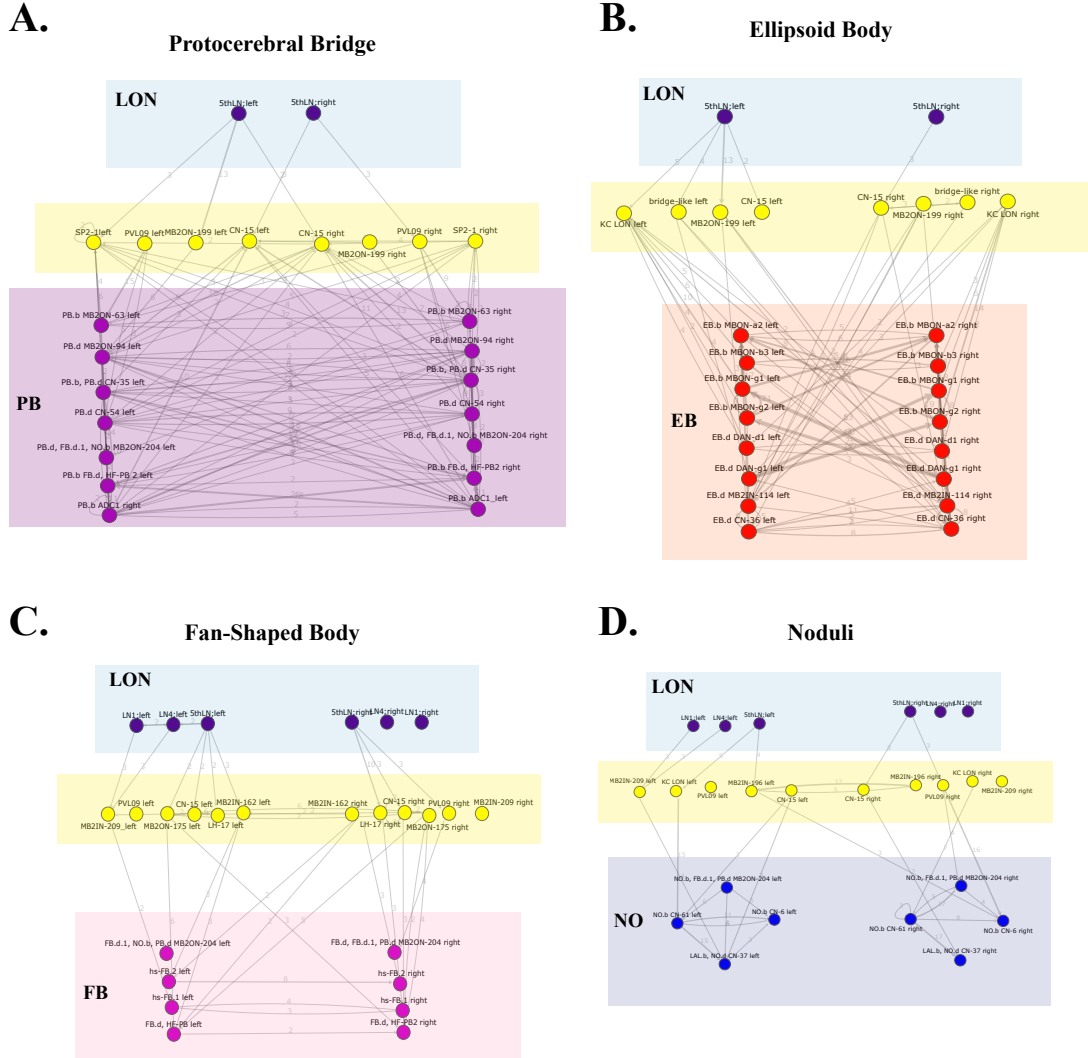


**Fig. 3.13 VLN Inputs to the Larval Central Complex.** The inputs from visual local interneurons (VLNs) towards each larval CX neuropil are shown. In each case, neurons are coloured to represent anatomical regions: VLNs are highlighted in a blue rectangle to represent the larval optic neuropil (LON), whilst the layer of interneurons connecting VLNs to the CX are highlighted in yellow. Individual CX neuropils are coloured in magenta (FB), red (EB), dark blue (NO), and deep purple (PB). In each case, both .d and .b neurons are included in the analysis. Panel A shows the VLN synaptic circuit towards the PB neurons; panel B displays the VLN synapses to EB neurons; panel C shows those to FB neurons; and panel D presents the VLN pathways towards the NO.

### 3.5 Descending Neurons from CX

To establish where central-complex neurons ultimately influence motor circuits, I traced all downstream partners of CX neurons and identified those whose axons descend into premotor compartments (SEZ and VNC). Descending neurons (DNs) were defined as neurons with a clear axonal projection leaving the subesophageal zone and coursing toward the subesophageal zone (SEZ) and/or the ventral nerve cord (VNC). Only synaptic partners with at least three output synapses from CX neurons were counted as meaningful CX to DNs links.

I found a set of 22 DNs that send presynapses (dendritic processes, therefore .d neurons) to CX neuropils, 9 of which are NO.d neurons, 4 EB.d neurons, 5 FB.d neurons and one pair of PB.d neurons (Table 3.10), annotated them as CX Descending. I then captured the 1st downstream layer of descending neurons from the CX (i.e DNs that are one hop away from CX, with one layer of interneurons; see second column of Table 3.10) and named these CX Descending 11. These were significantly more abundant (40 neurons), and interestingly many of the same .d neurons mentioned above appear here, suggesting recurrent connectivity between descending neurons.

CX Descending	CX Descending I1 (layer 1)
CX columnar system DPMm1 ipsilateral descending	A03o_a11
FB.d, FB.d.4, NO.d CM4 cen ant 1	A23f2 (= Pre-goro9)_a3l
EB-DN 1, EB.d, LAL-DN 1, LAL.d MB2ON-75	ascending to hairbrush and LBA3
DPMpm1 3	
DPMpm1 s 1	BAmd descending
DPMpm1 s 1	BAmv12 descending 1
FB.d, FB.d.5, NO.d, PB.d pitch;	BAmv12 descending 2
LAL output, LAL.d, NO.d DALd bushy	CM4 Bridle
NO.d ASB Gust descending	CM4 contralateral descending 1
NO.d BA1a34 lateral descending 1b	CP4 8
NO.d BA1p descending 1	DALcm12-v descending
NO.d BA1p descending 3	DPMI_ant_ven descending
NO.d BAm2_v descending	FAN-5, FB-10, MB2IN-11, MB2ON-19 AR ;
NO.d DPMI_ant_ven descending 3	FB-29, FBN-16, MB2IN-33, MB2ON-100 D
NO.d MB2IN-216 LAL to VNC up to A6	FB2IN-6, MB2IN-48, MB2ON-198 AS
NO.d MB2ON-200 CM4 ven pos 2	Horseshoe deviant
NO.d UNK descending 3	MB2IN-172 DPLc1 Descending
EB.d CN-36, FAN-4, FB-9, MB2IN-10, MB2ON-18 B	MB2IN-180 DNS-1
EB.d, FB.d MB2ON-17 Tomato Vine_	MB2IN-182 CSD
EB-MB 1, EB.d FB2IN-12, MB2IN-77 Mickey Mouse	MB2ON-4 BH ; Descending 2; CP1 v 2
FB.d CP descending contralateral 2	MB2ON-39 ipsigoro
FB.d, FB.d.1 DPMpm1 bushy descending	MB2ON-144 Tomato Vine 2
FB.d, FB.d.5, NO.d, PB.d pitch	MB2ON-205 DPLc_post_med descending
PB.d MIXED descending T	MB2ON-249 try5thLN_sibling 35
	mPN ginkgo 2
	NO-looper, NO.b BAmv12 looper 1
	NO.b CN-6, MB2ON-41 T5;
	NO.d ASB Gust descending
	NO.d BA1p descending 1
	NO.d BA1p descending 3
	NO.d DPMI_ant_ven descending 3
	NO.d MB2IN-216 LAL to VNC up to A6
	NO.d MB2ON-139 WD
	NO.d MB2ON-200 CM4 ven pos 2
	NO.d UNK descending 3
	EB.d CN-36, FAN-4, FB-9, MB2IN-10, MB2ON-18 B
	EB.d, FB.d MB2ON-17 Tomato Vine_
	EB-MB 1, EB.d FB2IN-12, MB2IN-77 Mickey Mouse
	FB.d CP descending contralateral 2
	FB.d, FB.d.1 DPMpm1 bushy descending
	FB.d, FB.d.5, NO.d, PB.d pitch
	PB.d MIXED descending T

Table 3.10 **CX Descending Neurons.** Descending neurons that either send dendrites to the CX (first column) or are one layer distance from the CX (second column) are shown. Highlighted cells indicate neurons whose activity has been screened via optogenetic stimulation.

Among these descending neurons, I found several that were optogenetically tested and, when activated, were shown to trigger specific motor behaviors (Table 3.11):

- NO.d DPMI\_ant\_ven descending 3 triggers backward crawling
- BAmd descending modulates turning
- MB2IN-172 DPLc1 Descending triggers stopping behaviour
- MB2ON-39 ipsigoro initiates forward crawling

Since one of the tested DNs is NO.d (DPMI\_ant\_ven descending 3) and triggers backward crawling, while the other behaviourally-tested DNs (BAmd descending, MB2IN-172, MB2ON-39) are one layer downstream from CX, this suggests direct involvement of the NO in motor behaviour, specifically backward locomotion. This aligns with the NO being the primary output area of the larval CX. The presence of additional DNs in the first downstream layer indicates that the CX can also influence motor behaviour through indirect pathways, particularly for turning, stopping, and forward crawling behaviors.

Overall, the fact that neurons directly influencing specific motor outputs receive input from CX neuropils suggests that the larval CX, like its adult counterpart, is involved in action selection and motor control.

Behaviour	CellType	Neuron Name	Split Line
Back	DN-VNC	NO.d DPMI_ant_ven descending 3	SS04603
Turn angle	DN-VNC	BAmd descending	SS01652
Stop	DN-SEZ	MB2IN-172 DPLc1 Descending	SS38042
Crawl	DN-VNC	MB2ON-39 ipsigoro	SS03731

Table 3.11 Descending neurons associated with specific behaviours and their split lines. Yellow cells highlight neuron and line pairs of interest.

## 3.6 Dopaminergic neurons (DANs) of the larval Central Complex

Dopaminergic release outside the MB in the adult fly is known to trigger sleep via dorsal FB (dFB) neurons (Pimentel et al., 2016), among other potential roles, depending upon the dopamine receptors expressed in the postsynaptic neurons and the circuits the neurons are part of.

The larval MB houses 7 pairs of DANs (Eichler et al., 2017), with several more DANs scattered across the brain (Selcho et al., 2009). By flip-out of the TH-GAL4 expression pattern that encompasses all DANs (Selcho et al., 2009) followed by immunohistochemistry, I isolated individual neurons from the TH-GAL4 expression pattern and compared their morphology with EM-reconstructed brain neurons (Winding et al., 2023). I identified with reasonable certainty the following 7 eDAN types (eDAN for *external* DAN, i.e., not a MB DAN), comprising 8 neuron pairs.

### 3.6.1 8 pairs of DANs outside of the MB

**eDAN-1:** from the larval lineage DPMpm2, this neuron presents an ipsilateral dendrite in the posterior-dorsal brain, and a bilateral axon exactly overlapping with HF-PB dendrites. eDAN-1 integrates inputs from PB.d neurons like CN-54 (which mediates multi-sensory input integration and relays them to HF-PB, modulated by MB output; see above) but also from multiple sensory PNs such as for temperature (Suckerfish PN, Thermo PN 3 and Thermo PN 5), olfaction (mPN A3), and for unknown sensory modalities (Suckerfish PN 2, from unknown sensory MN-Sens-B2-ACp-21 and -22; (Miroshnikow et al., 2018)), and also from PB.b neurons like MB2ON-63. The axon of eDAN-1 synapses onto multiple PB.d neurons (MB2ON-187, CN-15, CN-54, ADC1, FB-LAL1, and SP2-1) and weakly onto HF-PB neurons.

**eDAN-2:** from the larval lineage CM4-dm, this DAN presents a small, compact ipsilateral dendrite and a contralateral axon on the corresponding contralateral hemisphere right at the posterior end of the FB. eDAN-2 integrates inputs from FB neurons (strongly from FB.d.6, hs-FB.3, hs-FB.1, and weakly from many more). Its axon synapses onto MB2IN-195 (which is presynaptic to EB Wedge neurons), multiple FB neurons (hs-FB.3, hs-FB.1, FB.d.7 (FFN-6)), and weakly onto MB2IN-191 (the octopaminergic VUM of the CX).

**eDAN-3:** also known as MB2IN-139 (Eschbach et al., 2021), this neuron is from the larval lineage DPMpl12. Its dendrite is ipsilateral, sitting lateral to the FB but also extending into the LAL. The eDAN-3 axon targets a region dorsal to the LAL, housing the dendrites of many EB.d neurons onto which it synapses, such as MB2IN-114, EB-DN1, MB2ON-17, EB wedge neurons (only W1), and many more neurons such as convergence neurons (CN-30, CN-37, CN-38, CN-41, CN-42, CN-43), MB2ON-256, and a peculiar FB.d.1 neuron (Bushy).

**eDAN-4:** this type consists of two nearly identical neurons that share most inputs but differ only slightly in their outputs, since their axons are juxtaposed but tiled medio-laterally. From the larval lineage DPMpl12, they present an ipsilateral dendrite in the posterior ventral brain and a contralateral axon in the posterior intermediate brain, beyond the limits of the

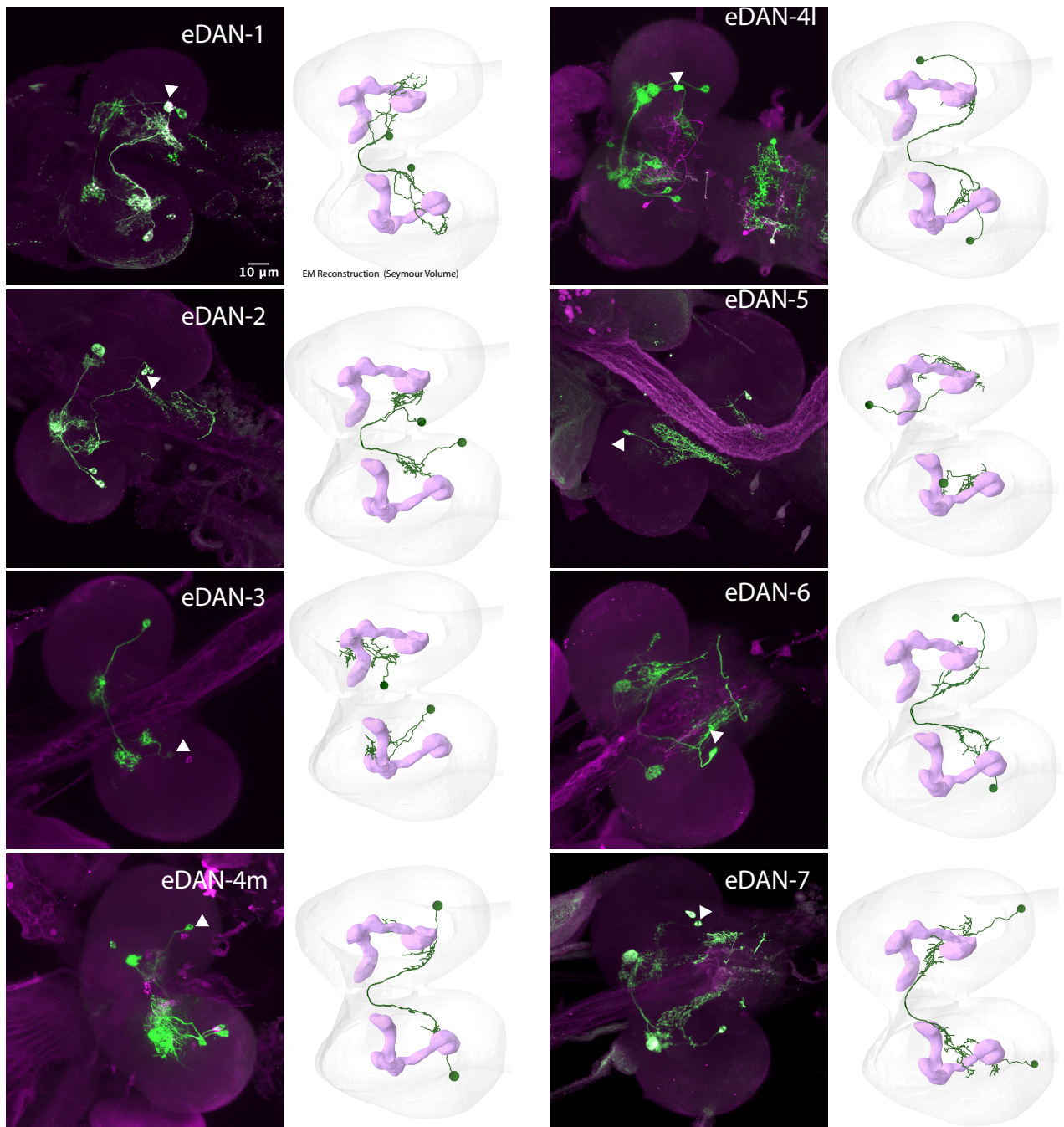


**Fig. 3.14 Immunostained Dopaminergic Neurons of non-MB neurons.** Representative TH-GAL4 flip-out labelled neurons in the Drosophila larval brain classified as central-complex dopaminergic neurons (eDANs). Three secondary antibodies were used, but only the channel showing the neuron of interest is displayed in each panel; the neuron signal is rendered green for consistency and background staining is tinted purple to improve contrast. Arrows mark the soma of the neuron of interest from a specific channel. On the right side of each confocal image, the EM 3D reconstruction of the corresponding neuron is shown.

FB proper. Both integrate inputs from numerous EB.d neurons like MB2IN-124, but only eDAN-41 (lateral axon) receives synapse from hs-FB.3. The axons of both eDAN-4 synapse onto some NO.d neurons like MB2ON-248 (whose dendrite has a domain in the NO and another outside where it meets the axon of both eDAN-4) and of other unidentified neurons (lasso-top 3, DALcm12-v descending), but only eDAN-41 synapses onto convergence neurons (CN-9, CN-26), and only eDAN-4m synapses onto hs-FB.5 and hs-FB.7.

**eDAN-5:** from the DPMpm1 larval lineage, this neuron's dendrite lays posterior to the LAL and projects its axon inside the lateral LAL. The dendrite integrates inputs from EB.d neurons, MB2IN-195, MB2ON-67, and sVUM2mx. The axon targets weakly but axo-dendritically an EB Ring neuron (RN1/2), and more strongly other neurons (MB2ON-67, MB2ON-78, MB2ON-68).

**eDAN-6:** Originating from the BLAvm larval lineage, this neuron (also known as SLR) presents a contralateral axon that spans both the FB and PB (therefore it is a PB.b FB.b), and notably targets PB horizontal fibres (HF-PB), and FB-NO1 neuron(which is an FB.d.1). This cell has an ipsilateral dendrite that integrates inputs from MB2ON-63, CN-9, and the FB intrinsic neuron MB2ON-175, in addition to a long tail of weaker input from ascending neurons relaying information from the somatosensory system.

**eDAN-7:** This neuron is a lateral horn neuron known as LH-LN2 (which stands for lateral horn local interneuron ??), originating from lineage BLP34. This neuron has an ipsilateral dendrite that integrates inputs from two CX core neurons: MB2ON-125, a local FB neuron(FB.d.b) and MB2IN-124 a local EB neuron (EB.d.b).

According to (Selcho et al., 2009) there are further non-MB DANs yet to be identified in the larval brain connectome. Note an effort was made to relate the eDANs I could identify to non-MB DAN names in (Selcho et al., 2009) but the resolution mismatch was too great to bridge, except for eDAN-1 which is most likely named "DM3" in (Selcho et al., 2009).

### 3.6.2 eDANs Connectivity

Whilst eDANs do not exhibit any significant interconnectivity, with the exception of eDAN-41 and eDAN-4m, all of CX neuropils receive direct input from these (Figure 3.15).

In the PB, ADC1(PB.b), HF-PB1 (PB.b), MBON-63(PB.b), CN-54(PB.d) and CN-4 (PB.d) all collect strong synaptic inputs from 6 separate DANs, suggesting dopaminergic modulation of neurons sending axonal processes to the PB as well as modulation of learning and memory inputs from the CNs. Notably, many PB neurons feed back onto these DANs.

The EB receives synaptic inputs from only 3 of eDANs, majority of which are eDAN-3. Notably, one wedge neuron (W1) which contributes both axons and dendrites to the EB (EB.d.b) collects strong synaptic inputs from eDAN3. Similarly, several EB.d neurons

(MB2ON-17, CN-43, and EB to LAL) all receive postsynapses from this eDAN. Interestingly, the EB to LAL neuron connects reciprocally to eDAN-4l and eDAN-5.

There are 3 tangential FB neurons (hs-FB.1, hs-FB.3 and hs-FB.5) receiving dopaminergic inputs from eDAN-2, eDAN-4l and eDAN4m, and recurrent connections from eDAN-2 to hs-FB.1 and hs-FB.3).

Finally, three neurons contributing dendrites to the NO(NO.d neurons) seem to both receive inputs from and send synapses to eDANs. CN-37 and MB2ON-248 receive synapses from eDAN-3 and eDAN-4l, respectively, whilst one MB2ON-35 sends synapses to eDAN3.

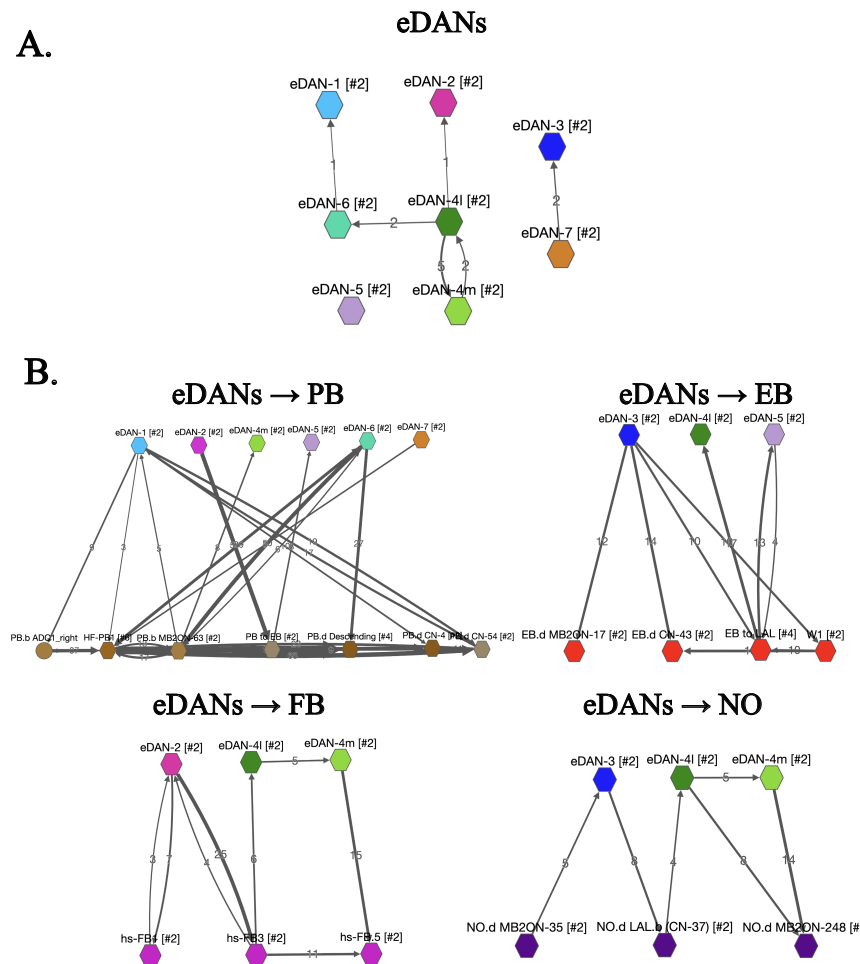


**Fig. 3.15 Connectivity between eDANs and the CX.** Panel A. displays the 8 eDANs connections to each other; panel B. presents direct downstream connections from eDANs to the CX neuropils (PB, EB, FB, NO)

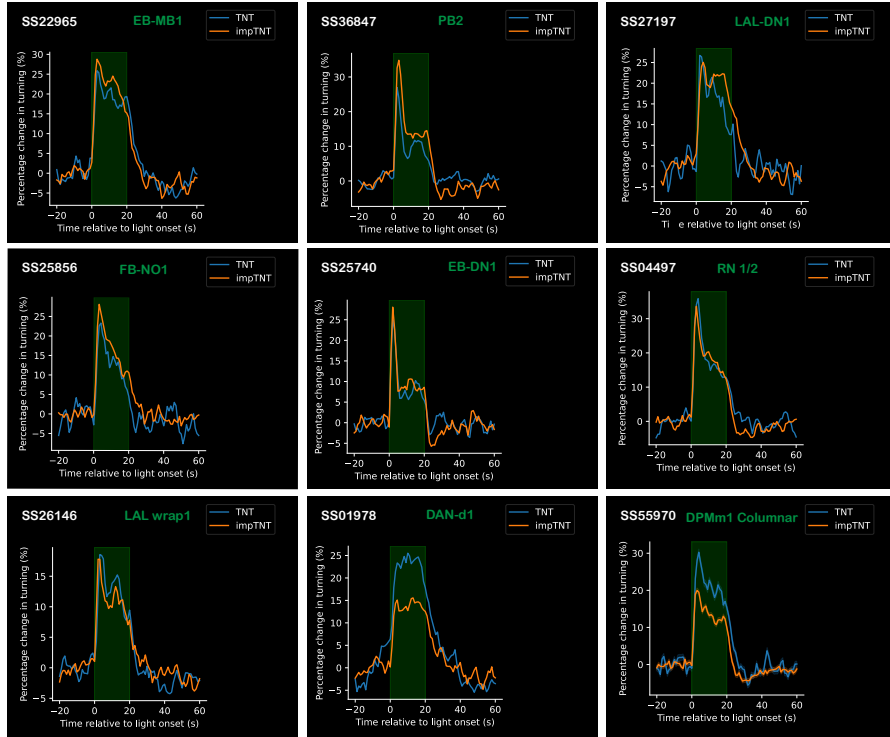


**Fig. 3.16 Loss-of-function Behavioural analysis of CX neurons expressing TNT and impTNT(disabled TNT)** The name of each split GAL4 line is written in white and their corresponding neuron name in green. Stimulation via green light is highlighted in green from 0-20s. The plots show a time-series of larvae's turning rates, coloured in blue for larvae expressing TNT and orange for larvae expressing impTNT

### 3.7 Behavioural Assays - Loss of Function Analysis during green Light stimulation

To probe the CX's role in visually-guided behaviors, I measured turning rates of larvae expressing TNT and impTNT in 9 distinct CX neurons during green light stimulation.

I identified genetic driver lines for nine neurons of the larval central complex: EB-MB1, PB2, LAL-DN1, LAL wrap1, FB-NO1, EB-DN1, RN1/2, plus DAN-d1, which is an EB.d (i.e., integrates inputs from the EB). I quantified larval turning behaviour following targeted inhibition of each of these driver lines via Tetanus neurotoxin (TNT). Control animals expressed the inactive variant, Impotent Tetanus (ImpTNT). Given that the central complex is classically implicated in visually guided navigation, I used green light stimulation as the sensory stimuli.

Neuron Name	Other names	Split Line	.b	.d	Lineage
DAN-d1	FB-33	SS01978		EB.d	CPb
LAL wrap 1	MB20N-116	SS26146		LAL.d	DALcl12-v
FB-NO 1		SS25856	NO.b	FB.d	DPMI12
EB-MB 1	FB2IN-12(Mickey Mouse)	SS22965		EB.d	BLP1/2
RN 1/2	FBN-20, MB2IN-38	SS04497	EB.b		DALv23
EB-DN 1	MB20N-75	SS25740		EB.d, LAL.d	DPMpm1
LAL-DN 1		SS27197		EB.d	DALd
PB2	PB horizontal fibres	SS36847	PB.b		Dalv1
DPMm1 Columnar	DPMm1 ipsilateral descending	SS55970			DPMm1

Table 3.12 **Neurons tested for LOF** Neuron names, corresponding split GAL4 line used for LOF experiments, and lineage information.

I found that expressing TNT did not show significant changes to turning rates for most neurons when compared to controls in response to green light stimulation, with the exception of DAN-d1 and DPMm1 Columnar 3.16.

DAN-d1, an EB.d neuron, showed significantly altered turning behaviour compared to controls. Similarly, DPMm1 Columnar, which is a descending neuron of the CX (see Table. 3.10) that was classified as columnar and synapses onto NO.d neurons, also seems to have visibly higher rates of turning compared to control.

While most CX neurons tested did not exhibit strong phenotypes individually this may reflect redundancy in the circuit or involvement in other aspects of visual processing beyond simple light avoidance. The selective effect of DAN-d1 manipulation suggests dopaminergic modulation of the EB may play a specific role in light-mediated behavioural responses. Further analysis is required into different types of behaviour for a complete understanding of their roles. Experiments with additional driver lines and behavioural paradigms would be needed to fully elucidate the functions of individual CX neurons in larval navigation.

## 3.8 Calcium Activity in response to Blue Light stimulation

I monitored the activity across the entire larval brain in response to stimulation of Rh5 (blue sensitive) photoreceptors. Photoreceptors (the Bolwig Organ) are located outside of the Central Nervous System(CNS) of Drosophila. I thus expressed EGFP fluorescent tag in these neurons(Rh5s) to ensure they are present during dissection of the CNS and that they are preserved for mounting the sample in the glass capillary prior to Calcium Imaging. I created a final line that expresses green fluorescent RGECHO (a calcium indicator of neural activity

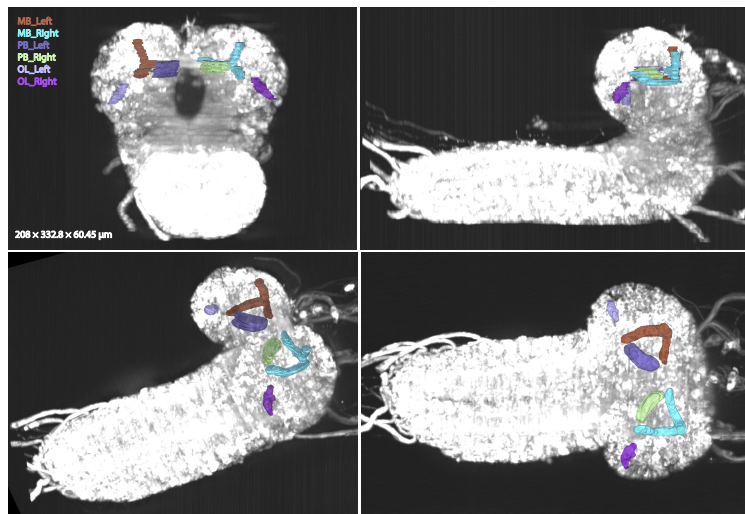


Fig. 3.17 Lightsheet Volume Segmentation

present cytosol) and red fluorescent IRFP (which brightens the cell nuclei very well and allows visualisation of cell position) and green fluorescent Rh5 photoreceptors.

Upon blue light stimulation, robust calcium transients in multiple regions of the larval brain were observed. Amongst the CX neuropils, I expected the neuropil with the most visual input (Protocerebral Bridge) to be reliably responsive to photoreceptor stimulation. To test this, the brain was segmented into distinct anatomical regions using manual annotation. Regions corresponding to the optic lobe (OL) - to confirm functional photoreceptors - the putative Protocerebral Bridge, and the MB - as a control - were delineated (Fig. 3.17) based on anatomical landmarks and lineage tracing data. Fluorescence intensity changes  $\Delta F/F_0$  were quantified for each region before, during and after blue light stimulation.

The Optic Lobe (OL) was reliably activated in response to light in sample 1,3 and 5 samples which confirms intact and functional photoreceptors. For sample 2 the left OL significantly less responsive than the right, indicating possible tissue damage on that side of the brain. Similarly for sample 4 the right side is less responsive than the left. Notably, across all samples, the OL exhibited a markedly larger  $\Delta F/F_0$  response compared to other regions of interest, creating a masking effect in data visualization. Specifically, the large amplitude of OL activity expanded the y-axis range, compressing the apparent variability in other regions and obscuring meaningful differences between the PB and the MB. To better resolve the relative dynamics among the remaining regions, the OL traces were excluded from subsequent analysis and the data was replotted and presented side by side with the original in figure 3.18.

When compared to the control (MB), the larval Protocerebral Bridge (PB) exhibited higher amplitude calcium transients in samples 2, 4, and 5, whereas both neuropils showed

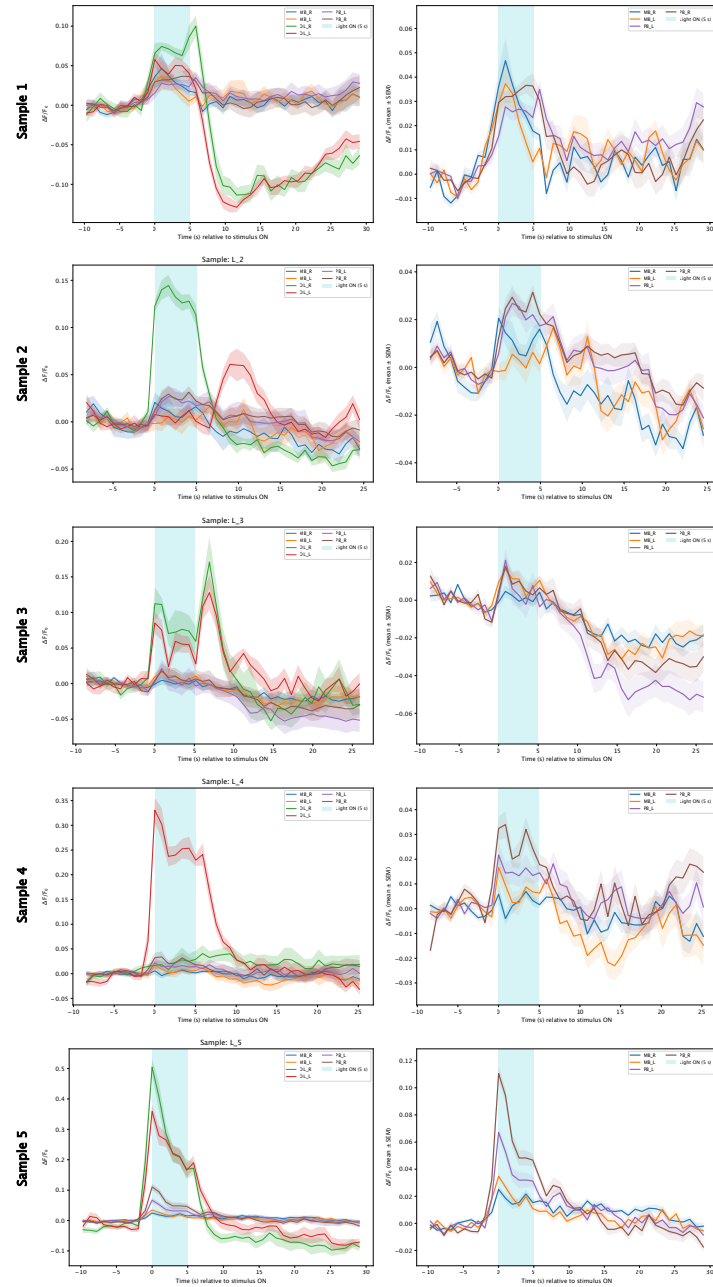


Fig. 3.18 Neural Activity of the Larval Brain in response to Photoreceptors Rh5 Stimulation

similar activity in samples 1 and 3. Interestingly, the two samples with one side of the optic lobe inactive (samples 2 and 4) displayed a more pronounced difference between PB and MB activity, suggesting that unilateral OL impairment may enhance the relative responsiveness of the PB to visual stimulation. This observation may indicate compensatory mechanisms or altered circuit dynamics in the presence of partial sensory deprivation. Overall, there seems to be a higher sensitivity to blue light from in PB compared to the MB, supporting the hypothesis of a functional role in visual input processing (Fig. 3.18). However, the effects aren't as significant as expected, possibly due to small sample size, suggesting the experiment could be underpowered.

# **Chapter 4**

## **Discussion**

Is there a Navigational Centre (Central Complex) in the Larval Drosophila?

The similarities between the larval Central Complex and the adult Central Complex PB,EB,FB,NO

Relation to accessory structures such as the LAL Sensory Biases: olfaction vs photoreception Central Complex relation to the Mushroom Body (Learning and Memory Centre of the fly) iii. Functions of the Larval central complex 1. Network connectivity predictions 2. Does biological data confirm our intuition? 3. Conclusions about the neural functionality iv. What we now know v. Expectations for the future vi. Can this teach us universal components of multisensory integration

### **4.1 Multisensory integration**

Gepner et al., 2015 demonstrated that Larvae have to integrate visual and olfactory gradients, with convergence of these sensory systems before decision to act on them. Exposed larvae to visual and olfactory input - blue light and optogenetic activation of appetitive ORNs No competition between types of taxis. multisensory integration happens immediately before the decision to navigate. Only one coherent representation Why is it that the information isn't processed at the time of decision making - i guess because command like neurons

### **4.2**

Our inquire into the nature of a fraction of neurons in the remaining *terra incognita* of the larval brain of the fruit fly yielded a series of neurons, neuropils and circuits with undeniable developmental, connectivity, and anatomical similarities to the set of core neuropils of

the central complex of the adult fly brain. The key anatomical difference of split brain hemispheres and the very early arrest of neuroblast proliferation in the larvae of Diptera impose strong constraints as to the extent of the anatomical and cellular similarities between the larval and the adult brain.

Notwithstanding, most larval brain neurons survive metamorphosis, help articulate homologous brain neuropils in the adult (Prieto-Godino et al., 2012), and participate of neural circuits in the adult brain. For example, the command neurons for backward locomotion (Carreira-Rosario et al., 2018), and MB MBINs and MBONs (Truman et al., 2023).

Intriguingly, while we find that larval brain neuronal lineages contribute the same neuronal cell types to the same CX neuropils as their corresponding adult brain instances do, we also find a number of neurons contributing to the larval CX that originate in non-CX lineages. This pattern has been reported before for the MB (Truman et al., 2023), with some larval MB neurons later on either undergoing apoptosis or, astonishingly, contributing to CX neuropils after metamorphosis. With the MB being an undeniably homologous structure to that of the adult and the larval Kenyon cells making up the bulk of the adult fly brain's gamma Kenyon cells, the recruitment of non-CX lineages into contributing CX neurons in the larva is perhaps part of a common theme in an animal with a limited neuron budget. The broader context being that the larva of the holometabola is derived (Truman & Riddiford, 2019, 1999), an evolutionary novelty that enabled this group of animals to exploit novel ecological niches that, to boot, avoids competition with the adults. In such predicament, it is perhaps not surprising that other larval neuropils similarly to the MB temporarily adopt neurons as their own that will eventually either perish by apoptosis or return to an ancestral cell fate away from the CX.

#### 4.2.1 Navigation, place learning, and memory

The central complex has been associated with place learning (for review see (Pfeiffer & Homberg, 2014)), with the EB in particular being necessary for visual place learning in flies (Ofstad et al., 2011). With fly larvae being capable of local search behavior (Kromp et al., 2024), the structure of the larval central complex and its close interactions with the center for associative memory, the mushroom body, must be examined.

We reported that the 'c' compartment of the larval MB is intimately associated with the FB. Intriguingly, MBON-c1 lacks a known role in associative memory to date, with all tests having been performed for olfactory associative memory (Eschbach et al., 2020). Likewise, we discovered a tight loop between the NO and the MB vertical lobe, by means of neurons that also lack a known function in learning: the multi-compartment MBON-p1, whose dendrites span across the MB vertical lobe, and MBIN-l1, a MB input neuron of

unknown neurotransmitter signature and function. Both of these MB compartments ought to be examined experimentally for potential roles in navigation or place learning.

With the NO having a role in the adult fly brain controlling the time course of walking activity (Strauss & Heisenberg, 1993) and in handedness in locomotion (Buchanan et al., 2015), and the larval MB vertical lobe mediating aversive memories (Eschbach et al., 2020), our report of a tight loop between the output of the MB vertical lobe and modulatory input onto it via the NO may provide the necessary corollary discharge to adjust MB operations to imminent locomotor activity, potentially laterally biased since both MBON-p1 and MBIN-l1 are both entirely ipsilateral-only neurons.

Furthermore, we found that the 'g' compartment of the MB, whose MBON-g1 and MBON-g2 promote avoidance (Eschbach et al., 2021) and its DAN-g1 is implicated in aversive learning (Eschbach et al., 2020), is intimately and recurrently associated with the Wedge and Ring neurons of the EB. Two further MBONs, MBON-a2 and MBON-b3, likewise synapse onto EB neurons. Among these, the function of MBON-b3 remains unknown. Intriguingly, both MBON-a2 and MBON-b3 are rare among the MBONs in having an ipsilateral-only dendrite but a bilateral axon, when the arborization pattern of MBONs is most often the opposite: bilateral dendrites and an ipsilateral axon. The ability of these MBONs to differentially discern sensory inputs between the left and right sides of the body is suggestive of a role in lateralized behavioral responses, such as in taxis.

In loss-of-function experiments, the suppression of DAN-d1 with TNT removes excitatory drive from MBON-d1, which is GABAergic (Eschbach et al., 2021). From the connectome we interpret that a neuron postsynaptic to MBON-d1, MB2ON-63, which is a PB horizontal fiber distinct from DALv1, will then receive less GABAergic input. And therefore, MB2ON-63 receives unopposed excitatory input from visual PNs (PVL09) and other excitatory visual neurons (ChalOLP), and from MBON-c1, all of which are cholinergic (Eschbach et al., 2021; Larderet et al., 2017). We speculate that, if in wild-type conditions the inhibition from the MB via MBON-d1 was potentially subtracting an expected intensity of light, to perform a temporal comparison, without it the animal would no longer be able to assert where the light has increased or decreased, leading to the need for continuing to sample by head casting or turning.

#### 4.2.2 DANs in the FB and PB

In the adult CX, dFB is a DAN that releases dopamine at the dorsal FB and is capable of triggering sleep (Pimentel et al., 2016). Intriguingly, we found a DAN (eDAN-2) among the FB intrinsic neurons, and two additional DANs (eDAN-4l and eDAN-4m) that synapse onto

a number of FB.d, FB.b and NO.d neurons. Identifying genetic driver lines for these neurons will enable testing experimentally their potential role in sleep regulation in larvae.

The role of eDAN-1, projecting to the larval PB, could be related to overall responsiveness and alertness of the animal, since there is a report that DANs projecting to the adult PB mediate increases in aggressiveness (Alekseyenko et al., 2013), and other DANs also projecting to the adult PB decrease sleep (Tomita et al., 2021).

What any of the identified non-MB DANs do awaits the identification of specific genetic driver lines and appropriate experimental setups to study their function.

#### 4.2.3 Conclusion

In conclusion, our interpretation of some of the until now underexamined larval brain circuits as a numerically reduced version of the adult fly central complex is coherent with the evolution of the larval stage in the Holometabola and with the known cell types and overall synaptic connectivity of the corresponding neuropils in adult fly brain, bringing a whole field of study into a life stage of reduced dimensions and numbers of neurons and synapses. Now, with our identification of tight circuit loops between understudied MB compartments and the larval CX, an opportunity opens to examine the neural circuit basis of spatial navigation and place learning in this experimentally tractable animal.

# References

- Ahrens, M. B., Orger, M. B., Robson, D. N., Li, J. M., & Keller, P. J. (2013). Whole-brain functional imaging at cellular resolution using light-sheet microscopy. *Nature methods*, 10(5), 413–420.
- Alekseyenko, O. V., Chan, Y.-B., Li, R., & Kravitz, E. A. (2013). Single dopaminergic neurons that modulate aggression in drosophila. *Proceedings of the National Academy of Sciences*, 110(15), 6151–6156.
- Almeida-Carvalho, M. J., Berh, D., Braun, A., Chen, Y.-c., Eichler, K., Eschbach, C., Fritsch, P. M., Gerber, B., Hoyer, N., Jiang, X., et al. (2017). The ol1mpiad: Concordance of behavioural faculties of stage 1 and stage 3 drosophila larvae. *Journal of Experimental Biology*, 220(13), 2452–2475.
- Andrade, I. V., Riebli, N., Nguyen, B.-C. M., Omoto, J. J., Cardona, A., & Hartenstein, V. (2019). Developmentally arrested precursors of pontine neurons establish an embryonic blueprint of the drosophila central complex. *Current Biology*, 29(3), 412–425.
- Berck, M. E., Khandelwal, A., Claus, L., Hernandez-Nunez, L., Si, G., Tabone, C. J., Li, F., Truman, J. W., Fetter, R. D., Louis, M., et al. (2016). The wiring diagram of a glomerular olfactory system. *Elife*, 5.
- Breitenfeld, T., Jurasic, M.-J., & Breitenfeld, D. (2014). Hippocrates: The forefather of neurology. *Neurological Sciences*, 35(9), 1349–1352.
- Brenner, S. (1974). The genetics of caenorhabditis elegans. *Genetics*, 77(1), 71–94.
- Buchanan, S. M., Kain, J. S., & De Bivort, B. L. (2015). Neuronal control of locomotor handedness in drosophila. *Proceedings of the National Academy of Sciences*, 112(21), 6700–6705.
- Carreira-Rosario, A., Zarin, A. A., Clark, M. Q., Manning, L., Fetter, R. D., Cardona, A., & Doe, C. Q. (2018). Mdn brain descending neurons coordinately activate backward and inhibit forward locomotion. *Elife*, 7, e38554.
- Davies, A., Louis, M., & Webb, B. (2015). A model of drosophila larva chemotaxis. *PLoS computational biology*, 11(11), e1004606.
- Donlea, J. M. (2019). Roles for sleep in memory: Insights from the fly. *Current opinion in neurobiology*, 54, 120–126.
- Donlea, J. M., Thimgan, M. S., Suzuki, Y., Gottschalk, L., & Shaw, P. J. (2011). Inducing sleep by remote control facilitates memory consolidation in drosophila. *Science*, 332(6037), 1571–1576.
- Ebrahim, S. A., Dweck, H. K., Stökl, J., Hofferberth, J. E., Trona, F., Weniger, K., Rybak, J., Seki, Y., Stensmyr, M. C., Sachse, S., et al. (2015). Drosophila avoids parasitoids by sensing their semiochemicals via a dedicated olfactory circuit. *PLoS biology*, 13(12), e1002318.

- Eckstein, N., Bates, A. S., Champion, A., Du, M., Yin, Y., Schlegel, P., Lu, A. K.-Y., Rymer, T., Finley-May, S., Paterson, T., et al. (2024). Neurotransmitter classification from electron microscopy images at synaptic sites in drosophila melanogaster. *Cell*, 187(10), 2574–2594.
- Eichler, K., Li, F., Litwin-Kumar, A., Park, Y., Andrade, I., Schneider-Mizell, C. M., Saumweber, T., Huser, A., Eschbach, C., Gerber, B., et al. (2017). The complete connectome of a learning and memory centre in an insect brain. *Nature*, 548(7666), 175–182.
- Eschbach, C., Fushiki, A., Winding, M., Afonso, B., Andrade, I. V., Cocanougher, B. T., Eichler, K., Gepner, R., Si, G., Valdes-Aleman, J., et al. (2021). Circuits for integrating learned and innate valences in the insect brain. *Elife*, 10, e62567.
- Eschbach, C., Fushiki, A., Winding, M., Schneider-Mizell, C. M., Shao, M., Arruda, R., Eichler, K., Valdes-Aleman, J., Ohyama, T., Thum, A. S., et al. (2020). Recurrent architecture for adaptive regulation of learning in the insect brain. *Nature neuroscience*, 23(4), 544–555.
- Farnsworth, M. S., Bucher, G., & Hartenstein, V. (2022). An atlas of the developing triatomum castaneum brain reveals conservation in anatomy and divergence in timing to drosophila melanogaster. *Journal of Comparative Neurology*, 530(13), 2335–2371.
- Farnsworth, M. S., Eckermann, K. N., & Bucher, G. (2020). Sequence heterochrony led to a gain of functionality in an immature stage of the central complex: A fly-beetle insight. *PLoS biology*, 18(10), e3000881.
- Fisher, Y. E. (2022). Flexible navigational computations in the drosophila central complex. *Current opinion in neurobiology*, 73, 102514.
- Fishilevich, E., Domingos, A. I., Asahina, K., Naef, F., Vosshall, L. B., & Louis, M. (2005). Chemotaxis behavior mediated by single larval olfactory neurons in drosophila. *Current biology*, 15(23), 2086–2096.
- Franconville, R., Beron, C., & Jayaraman, V. (2018). Building a functional connectome of the drosophila central complex. *Elife*, 7, e37017.
- Functional connectomics spanning multiple areas of mouse visual cortex. (2025). *Nature*, 640(8058), 435–447.
- Gepner, R., Mihovilovic Skanata, M., Bernat, N. M., Kaplow, M., & Gershaw, M. (2015). Computations underlying drosophila photo-taxis, odor-taxis, and multi-sensory integration. *Elife*, 4, e06229.
- Gerhard, S., Andrade, I., Fetter, R. D., Cardona, A., & Schneider-Mizell, C. M. (2017). Conserved neural circuit structure across drosophila larval development revealed by comparative connectomics. *Elife*, 6, e29089.
- Gong, Z. (2009). Behavioral dissection of drosophila larval phototaxis. *Biochemical and Biophysical Research Communications*, 382(2), 395–399.
- Goodman, C. S., Bastiani, M. J., Doe, C. Q., Du Lac, S., Helfand, S. L., Kuwada, J. Y., & Thomas, J. B. (1984). Cell recognition during neuronal development. *Science*, 225(4668), 1271–1279.
- Hanesch, U., Fischbach, K.-F., & Heisenberg, M. (1989). Neuronal architecture of the central complex in drosophila melanogaster. *Cell and Tissue Research*, 257(2), 343–366.
- Heinze, S. (2017). Unraveling the neural basis of insect navigation. *Current opinion in insect science*, 24, 58–67.
- Heinze, S. (2024). Variations on an ancient theme—the central complex across insects. *Current Opinion in Behavioral Sciences*, 57, 101390.

- Heinze, S., Gotthardt, S., & Homberg, U. (2009). Transformation of polarized light information in the central complex of the locust. *Journal of Neuroscience*, 29(38), 11783–11793.
- Heinze, S., Narendra, A., & Cheung, A. (2018). Principles of insect path integration. *Current Biology*, 28(17), R1043–R1058.
- Herculano-Houzel, S. (2009). The human brain in numbers: A linearly scaled-up primate brain. *Frontiers in human neuroscience*, 3, 857.
- Hernandez-Nunez, L., Chen, A., Budelli, G., Berck, M. E., Richter, V., Rist, A., Thum, A. S., Cardona, A., Klein, M., Garrity, P., et al. (2021). Synchronous and opponent thermosensors use flexible cross-inhibition to orchestrate thermal homeostasis. *Science advances*, 7(35), eabg6707.
- Honkanen, A., Adden, A., da Silva Freitas, J., & Heinze, S. (2019). The insect central complex and the neural basis of navigational strategies. *Journal of Experimental Biology*, 222(Suppl\_1), jeb188854.
- Huang, L., Kebischull, J. M., Fürth, D., Musall, S., Kaufman, M. T., Churchland, A. K., & Zador, A. M. (2020). Bricseq bridges brain-wide interregional connectivity to neural activity and gene expression in single animals. *Cell*, 182(1), 177–188.
- Hückesfeld, S., Schlegel, P., Mirochnikow, A., Schoofs, A., Zinke, I., Haubrich, A. N., Schneider-Mizell, C. M., Truman, J. W., Fetter, R. D., Cardona, A., et al. (2021). Unveiling the sensory and interneuronal pathways of the neuroendocrine connectome in drosophila. *Elife*, 10, e65745.
- Hulse, B. K., Haberkern, H., Franconville, R., Turner-Evans, D. B., Takemura, S.-y., Wolff, T., Noorman, M., Dreher, M., Dan, C., Parekh, R., et al. (2021). A connectome of the drosophila central complex reveals network motifs suitable for flexible navigation and context-dependent action selection. *ELife*, 10, e66039.
- Humberg, T.-H., Bruegger, P., Afonso, B., Zlatic, M., Truman, J. W., Gershow, M., Samuel, A., & Sprecher, S. G. (2018). Dedicated photoreceptor pathways in drosophila larvae mediate navigation by processing either spatial or temporal cues. *Nature communications*, 9(1), 1260.
- Jacobs, J. R., & Goodman, C. S. (1989). Embryonic development of axon pathways in the drosophila CNS. II. Behavior of pioneer growth cones. *Journal of Neuroscience*, 9(7), 2412–2422.
- Kahsai, L., Carlsson, M. A., Winther, Å. M., & Nässel, D. R. (2012). Distribution of metabotropic receptors of serotonin, dopamine, gaba, glutamate, and short neuropeptide f in the central complex of drosophila. *Neuroscience*, 208, 11–26.
- Kahsai, L., & Winther, Å. M. (2011). Chemical neuroanatomy of the drosophila central complex: Distribution of multiple neuropeptides in relation to neurotransmitters. *Journal of Comparative Neurology*, 519(2), 290–315.
- Keene, A. C., Mazzoni, E. O., Zhen, J., Younger, M. A., Yamaguchi, S., Blau, J., Desplan, C., & Sprecher, S. G. (2011). Distinct visual pathways mediate drosophila larval light avoidance and circadian clock entrainment. *Journal of Neuroscience*, 31(17), 6527–6534.
- Keene, A. C., & Sprecher, S. G. (2012). Seeing the light: Photobehavior in fruit fly larvae. *Trends in neurosciences*, 35(2), 104–110.
- Khurana, S., & Siddiqi, O. (2013). Olfactory responses of drosophila larvae. *Chemical senses*, 38(4), 315–323.

- Kim, S. S., Franconville, R., Turner-Evans, D., & Jayaraman, V. (2015). Optogenetics in *drosophila melanogaster*. In *New techniques in systems neuroscience* (pp. 147–176). Springer.
- Koniszewski, N. D. B., Kollmann, M., Bigham, M., Farnworth, M., He, B., Büscher, M., Hütteroth, W., Binzer, M., Schachtner, J., & Bucher, G. (2016). The insect central complex as model for heterochronic brain development—background, concepts, and tools. *Development genes and evolution*, 226(3), 209–219.
- Kromp, J., Triphan, T., & Thum, A. S. (2024). Finding a path: Local search behavior of *drosophila* larvae. *bioRxiv*, 2024–11.
- Lacin, H., & Truman, J. W. (2016). Lineage mapping identifies molecular and architectural similarities between the larval and adult *drosophila* central nervous system. *Elife*, 5, e13399.
- Lai, S.-L., Awasaki, T., Ito, K., & Lee, T. (2008). Clonal analysis of *drosophila* antennal lobe neurons: Diverse neuronal architectures in the lateral neuroblast lineage.
- Larderet, I., Fritsch, P. M., Gendre, N., Neagu-Maier, G. L., Fetter, R. D., Schneider-Mizell, C. M., Truman, J. W., Zlatic, M., Cardona, A., & Sprecher, S. G. (2017). Organization of the *drosophila* larval visual circuit. *Elife*, 6, e28387.
- Lemon, W. C., Pulver, S. R., Höckendorf, B., McDole, K., Branson, K., Freeman, J., & Keller, P. J. (2015). Whole-central nervous system functional imaging in larval *drosophila*. *Nature communications*, 6(1), 7924.
- Li, H.-H., Kroll, J. R., Lennox, S. M., Ogundeyi, O., Jeter, J., Depasquale, G., & Truman, J. W. (2014). A gal4 driver resource for developmental and behavioral studies on the larval cns of *drosophila*. *Cell reports*, 8(3), 897–908.
- Lin, C.-Y., Chuang, C.-C., Hua, T.-E., Chen, C.-C., Dickson, B. J., Greenspan, R. J., & Chiang, A.-S. (2013). A comprehensive wiring diagram of the protocerebral bridge for visual information processing in the *drosophila* brain. *Cell reports*, 3(5), 1739–1753.
- Lovick, J. K., Ngo, K. T., Omoto, J. J., Wong, D. C., Nguyen, J. D., & Hartenstein, V. (2013). Postembryonic lineages of the *drosophila* brain: I. development of the lineage-associated fiber tracts. *Developmental Biology*, 384(2), 228–257.
- Mast, J. D., De Moraes, C. M., Alborn, H. T., Lavis, L. D., & Stern, D. L. (2014). Evolved differences in larval social behavior mediated by novel pheromones. *Elife*, 3, e04205.
- McKinstry-Wu, A. R., & Kelz, M. B. (2013). Connectome: How the brain's wiring makes us who we are. *Anesthesia & Analgesia*, 117(6), 1513–1514.
- Meinertzhagen, I. A. (2016). Connectome studies on *drosophila*: A short perspective on a tiny brain. *Journal of neurogenetics*, 30(2), 62–68.
- Meissner, G. W., Vannan, A., Jeter, J., Close, K., DePasquale, G. M., Dorman, Z., Forster, K., Beringer, J. A., Gibney, T., Hausenfluck, J. H., et al. (2025). A split-gal4 driver line resource for *drosophila* neuron types. *elife*, 13, RP98405.
- Miroschnikow, A., Schlegel, P., Schoofs, A., Hueckesfeld, S., Li, F., Schneider-Mizell, C. M., Fetter, R. D., Truman, J. W., Cardona, A., & Pankratz, M. J. (2018). Convergence of monosynaptic and polysynaptic sensory paths onto common motor outputs in a *drosophila* feeding connectome. *Elife*, 7, e40247.
- Nern, A., Pfeiffer, B. D., & Rubin, G. M. (2015). Optimized tools for multicolor stochastic labeling reveal diverse stereotyped cell arrangements in the fly visual system. *Proceedings of the National Academy of Sciences*, 112(22), E2967–E2976.
- Ofstad, T. A., Zuker, C. S., & Reiser, M. B. (2011). Visual place learning in *drosophila melanogaster*. *Nature*, 474(7350), 204–207.

- Ohyama, T., Jovanic, T., Denisov, G., Dang, T. C., Hoffmann, D., Kerr, R. A., & Zlatic, M. (2013). High-throughput analysis of stimulus-evoked behaviors in drosophila larva reveals multiple modality-specific escape strategies. *PloS one*, 8(8), e71706.
- Ohyama, T., Schneider-Mizell, C. M., Fetter, R. D., Aleman, J. V., Franconville, R., Rivera-Alba, M., Mensh, B. D., Branson, K. M., Simpson, J. H., Truman, J. W., et al. (2015). A multilevel multimodal circuit enhances action selection in drosophila. *Nature*, 520(7549), 633–639.
- Omoto, J. J., Keleş, M. F., Nguyen, B.-C. M., Bolanos, C., Lovick, J. K., Frye, M. A., & Hartenstein, V. (2017). Visual input to the drosophila central complex by developmentally and functionally distinct neuronal populations. *Current Biology*, 27(8), 1098–1110.
- Omoto, J. J., Nguyen, B.-C. M., Kandimalla, P., Lovick, J. K., Donlea, J. M., & Hartenstein, V. (2018). Neuronal constituents and putative interactions within the drosophila ellipsoid body neuropil. *Frontiers in neural circuits*, 12, 103.
- Owald, D., Lin, S., & Waddell, S. (2015). Light, heat, action: Neural control of fruit fly behaviour. *Philosophical Transactions of the Royal Society B: Biological Sciences*, 370(1677), 20140211.
- Pereanu, W., Kumar, A., Jennett, A., Reichert, H., & Hartenstein, V. (2010). Development-based compartmentalization of the drosophila central brain. *Journal of Comparative Neurology*, 518(15), 2996–3023.
- Pereanu, W., Younossi-Hartenstein, A., Lovick, J., Spindler, S., & Hartenstein, V. (2011). Lineage-based analysis of the development of the central complex of the *Drosophila* brain. *Journal of Comparative Neurology*, 519(4), 661–689.
- Pfeiffer, K., & Homberg, U. (2014). Organization and functional roles of the central complex in the insect brain. *Annual review of entomology*, 59(1), 165–184.
- Pimentel, D., Donlea, J. M., Talbot, C. B., Song, S. M., Thurston, A. J., & Miesenböck, G. (2016). Operation of a homeostatic sleep switch. *Nature*, 536(7616), 333–337.
- Pisokas, I., Heinze, S., & Webb, B. (2020). The head direction circuit of two insect species. *Elife*, 9, e53985.
- Poe, A. R., Zhu, L., Szuperak, M., McClanahan, P. D., Anafi, R. C., Scholl, B., Thum, A. S., Cavanaugh, D. J., & Kayser, M. S. (2023). Developmental emergence of sleep rhythms enables long-term memory in drosophila. *Science Advances*, 9(36), eadh2301.
- Prieto-Godino, L. L., Diegelmann, S., & Bate, M. (2012). Embryonic origin of olfactory circuitry in drosophila: Contact and activity-mediated interactions pattern connectivity in the antennal lobe.
- Saalfeld, S., Cardona, A., Hartenstein, V., & Tomančák, P. (2009). Catmaid: Collaborative annotation toolkit for massive amounts of image data. *Bioinformatics*, 25(15), 1984–1986.
- Sawin-McCormack, E. P., Sokolowski, M. B., & Campos, A. R. (1995). Characterization and genetic analysis of drosophila melanogaster photobehavior during larval development. *Journal of neurogenetics*, 10(2), 119–135.
- Scheffer, L. K., Xu, C. S., Januszewski, M., Lu, Z., Takemura, S.-y., Hayworth, K. J., Huang, G. B., Shinomiya, K., Maitlin-Shepard, J., Berg, S., et al. (2020). A connectome and analysis of the adult drosophila central brain. *elife*, 9, e57443.
- Schlegel, P., Texada, M. J., Mirochnikow, A., Schoofs, A., Hückesfeld, S., Peters, M., Schneider-Mizell, C. M., Lacin, H., Li, F., Fetter, R. D., et al. (2016). Synaptic

- transmission parallels neuromodulation in a central food-intake circuit. *Elife*, 5, e16799.
- Schneider-Mizell, C. M., Gerhard, S., Longair, M., Kazimiers, T., Li, F., Zwart, M. F., Champion, A., Midgley, F. M., Fetter, R. D., Saalfeld, S., et al. (2016). Quantitative neuroanatomy for connectomics in drosophila. *Elife*, 5, e12059.
- Seelig, J. D., & Jayaraman, V. (2013). Feature detection and orientation tuning in the drosophila central complex. *Nature*, 503(7475), 262–266.
- Seelig, J. D., & Jayaraman, V. (2015). Neural dynamics for landmark orientation and angular path integration. *Nature*, 521(7551), 186–191.
- Selcho, M., Pauls, D., Han, K.-A., Stocker, R. F., & Thum, A. S. (2009). The role of dopamine in drosophila larval classical olfactory conditioning. *PloS one*, 4(6), e5897.
- Shafer, O. T., & Keene, A. C. (2021). The regulation of *Drosophila* sleep. *Current Biology*, 31(1), R38–R49.
- Spindler, S. R., & Hartenstein, V. (2010). The drosophila neural lineages: A model system to study brain development and circuitry. *Development genes and evolution*, 220(1), 1–10.
- Stone, T., Webb, B., Adden, A., Weddig, N. B., Honkanen, A., Templin, R., Wcislo, W., Scimeca, L., Warrant, E., & Heinze, S. (2017). An anatomically constrained model for path integration in the bee brain. *Current Biology*, 27(20), 3069–3085.
- Strauss, R., & Heisenberg, M. (1993). A higher control center of locomotor behavior in the drosophila brain. *Journal of Neuroscience*, 13(5), 1852–1861.
- Szuperak, M., Churgin, M. A., Borja, A. J., Raizen, D. M., Fang-Yen, C., & Kayser, M. S. (2018). A sleep state in drosophila larvae required for neural stem cell proliferation. *Elife*, 7, e33220.
- Tomita, J., Ban, G., Kato, Y. S., & Kume, K. (2021). Protocerebral bridge neurons that regulate sleep in drosophila melanogaster. *Frontiers in Neuroscience*, 15, 647117.
- Truman, J. W., Price, J., Miyares, R. L., & Lee, T. (2023). Metamorphosis of memory circuits in drosophila reveals a strategy for evolving a larval brain. *Elife*, 12, e80594.
- Truman, J. W., & Riddiford, L. M. (2019). The evolution of insect metamorphosis: A developmental and endocrine view. *Philosophical Transactions of the Royal Society B*, 374(1783), 20190070.
- Truman, J. W., & Riddiford, L. M. (1999). The origins of insect metamorphosis. *Nature*, 401(6752), 447–452.
- Turner-Evans, D. B., & Jayaraman, V. (2016). The insect central complex. *Current Biology*, 26(11), R453–R457.
- Vogelstein, J. T., Park, Y., Ohya, T., Kerr, R. A., Truman, J. W., Priebe, C. E., & Zlatic, M. (2014). Discovery of brainwide neural-behavioral maps via multiscale unsupervised structure learning. *Science*, 344(6182), 386–392.
- Vogt, K., Zimmerman, D. M., Schlichting, M., Hernandez-Nunez, L., Qin, S., Malacon, K., Rosbash, M., Pehlevan, C., Cardona, A., & Samuel, A. D. (2021). Internal state configures olfactory behavior and early sensory processing in drosophila larvae. *Science advances*, 7(1), eabd6900.
- Winding, M., Pedigo, B. D., Barnes, C. L., Patsolic, H. G., Park, Y., Kazimiers, T., Fushiki, A., Andrade, I. V., Khandelwal, A., Valdes-Aleman, J., et al. (2023). The connectome of an insect brain. *Science*, 379(6636), eadd9330.
- Wolff, T., Iyer, N. A., & Rubin, G. M. (2015). Neuroarchitecture and neuroanatomy of the drosophila central complex: A gal4-based dissection of protocerebral bridge neurons and circuits. *Journal of Comparative Neurology*, 523(7), 997–1037.

- Wolff, T., & Rubin, G. M. (2018). Neuroarchitecture of the drosophila central complex: A catalog of nodulus and asymmetrical body neurons and a revision of the protocerebral bridge catalog. *Journal of Comparative Neurology*, 526(16), 2585–2611.
- Yang, J. S., Awasaki, T., Yu, H.-H., He, Y., Ding, P., Kao, J.-C., & Lee, T. (2013). Diverse neuronal lineages make stereotyped contributions to the drosophila locomotor control center, the central complex. *Journal of Comparative Neurology*, 521(12), 2645–2662.
- Zheng, Z., Lauritzen, J. S., Perlman, E., Robinson, C. G., Nichols, M., Milkie, D., Torrens, O., Price, J., Fisher, C. B., Sharifi, N., et al. (2018). A complete electron microscopy volume of the brain of adult drosophila melanogaster. *Cell*, 174(3), 730–743.

